Addis Ababa University

Addis Ababa Institute of Technology

School of Chemical and Bio Engineering

Synthesis and Performance Evaluation of Titanium Dioxide Supported Bentonite Composite for Methyl Orange Removal from Wastewater

Abrham Balew Jemberie

MSc Thesis

A Thesis Submitted to the School of Chemical and Bio Engineering, Addis Ababa Institute of Technology, Addis Ababa University in partial fulfillment of the requirements for the attainment of the degree of Master of Science in Chemical Engineering (Process Engineering)

Addis Ababa University

Addis Ababa, Ethiopia

June, 2019

Addis Ababa University

Addis Ababa Institute of Technology

School of Chemical and Bio Engineering

This is to certify that the thesis prepared by Abrham Balew, entitled with "*Synthesis and performance evaluation of titanium dioxide supported bentonite composite for methyl orange removal in waste water*" and submitted in partial fulfillment of the requirements for the degree of Masters of Science in Chemical and Bio Engineering (Process engineering) complies with the regulation of the university and meets the accepted standards with respect to originality and quality.

Approved by the Examining Board:

Dr. Abubeker Yimam		
Head of School of Chemical and Bio Engineering	Signature	Date
Dr. Shimelis Kebede		
Advisor	Signature	Date
Dr. Berhanu Assefa		
Internal Examiner	Signature	Date
Ato. Teshome Worku		
External Examiner	Signature	Date

DECLARATION

I declare that this MSc thesis entitled "*Synthesis and performance evaluation of titanium dioxide supported bentonite composite for methyl orange removal in waste water*" is my original work and has not previously submitted by others in this university and other universities. However contributions of others are included, for further clarification of literatures and discussions. And the information is taken from published and unpublished works of others has been acknowledged in the text and listed in the reference.

Name: Abrham Balew

Signature: _____

This thesis has been submitted for examination with my approval as university advisor.

Name: Dr. Shimels Kebede

Signature: _____

Date: _____

ACKNOWLEDGMENT

First and foremost, I would like to thank the almighty God who has given health and strength to complete my thesis. Next I would like to express my gratitude to my advisor, Dr. Shimels Kebede for his valuable guidance, encouragement and supervision starting from proposal development and throughout my MSc studies. Also I would like to thank Dr. Beteley Tekola Associate Director for Research at AAiT for his role in providing bentonite clay collected from Afar region for my experimental work. Additionally, I would like to acknowledge AAiT, School of Chemical and Bio-engineering lab assistants for their kind technical support throughout my laboratory work. I'm deeply grateful for my families and friends for their continuous support and encouragement. Finally, I would like to thank AAU, Natural and Computational College for their cooperation.

ABSTRACT

Dye effluents discharged from different industries causes series damage to aquatic animals as well as human beings by mutagenic and carcinogenic effects. Thus, the effluents needs to be treated before discharged to the environment using advanced oxidation process. TiO_2 supported bentonite composite was used in the photocatalytic discoloration of dyes from wastewater i.e., methyl orange (MO). During usage of the composite as a photocatalyst for dye removal, physiochemical characteristics and effect of synthesis and photocatalytic parameters were investigated using Box-Behnkon Design response surface methodology. Characterization of the composite catalyst XRD analysis revealed that, the composite catalyst contains bentonite component (montmorillonite, quartz and feldspar) and TiO_2 components (anatase and rutile). The crystal size of raw bentonite and composite were 24.73nm and 53.43nm respectively. In the design of experiment, the efficient catalyst was selected based on its dye removal efficiency via numerical optimization. Calcination temperature $400^{O}C$, calcination time 2h and TiO_2 to bentonite ratio 0.2 were selected for 96.54% removal efficiency. Also for photocatalytic experiment dye concentration 10mg/L, catalyst dose 1.5g/L and UV irradiation time 2h gave 94.88% removal efficiency. The study justified that, composite photocatalyst titanium dioxide supported with bentonite has many advantages such as improve photocatalytic efficiency, recycling efficiency of the catalyst, improves the recovery rate, save the cost of treatment and improves the light absorption efficiency.

Key words: *Impregnation; Composite; Photocatalysis; Methyl orange; Box-Behnkon Design*

TABLE OF CONTENTS

LIST OF FIGURES

LIST OF TABLES

LIST OF ABBREVIATIONS

BOD	Biochemical Oxygen Demand
COD	Chemical Oxygen Demand
AOP	Advanced oxidation process
UV	Ultraviolet
MO	Methyl Orange
RSM	Response Surface Methodology
ANOVA	Analysis of variance
BBD	Box Behenken Design
XRD	X-ray diffraction
FTIR	Fourier Transform Infrared Radiat
IPCA	Integrated Photocatalytic Adsorbent
JCPDS	Joint Committee on Powder Diffraction Standards
ICDD	International Center for Diffraction Data

Chapter 1

INTRODUCTION

1.1. Background

Water is a precious resource that is important to every living thing throughout the world. Water covered almost 70 percent on the earth but only 2.5 % is indicated as fresh water (Yahya et al., 2018). In recent years, the arising ecological problems connected with the presence of potentially carcinogenic compounds have been widely observed. In addition, these dangerous compounds are often non-biodegradable or toxic to microorganisms and have very long degradation time in the environment (Sun et al., 2002). The situation is alarming because of the lack of adequate wastewater treatment technologies capable of reducing the toxic substances that present in a persistent chemical risk. There are ample treatment technologies for sewage, distillery effluents and so on, which contain biodegradable organics, but not so much for toxic effluents containing xenobiotic compounds, which are often non-biodegradable or only partially biodegradable (X. P. Wu, 2017).

There are different types of water pollutants which causes pollutions such as: organic pollutants, pathogens, nutrient, agriculture runoff, suspended solids and sediments (organic and inorganic), inorganic pollutants (salt and metals), thermal pollution and radioactive pollutants. Organic pollutants can be further classified as: oxygen demanding wastes, synthetic organic compounds and oils (Leu, 2006). Water pollution due to effluents from textile dyeing industry is a cause of serious concern. The techniques for detection of dyes are cost intensive and futile because the dyes undergo chemical changes under environmental conditions and the transformation products may be more toxic and carcinogenic than the parent molecule (Padhi, 2012).

Textile dyes and other industrial dyestuffs constitute one of the largest groups of organic compounds that represent an increasing environmental danger (Konstantinou & Albanis, 2004). About 15% of total global dye production is lost during the dyeing process and released in textile effluents. The release of those colored waste waters into the ecosystem is a substantial source of non-aesthetic pollution (Laysandra, Sari, et al., 2017). Waste water from textile, paper and some other industrial processes are usually highly colored, toxic, carcinogenic or mutagenic.

Dyes usually have complex aromatic molecular structures which make them more stable and difficult to biodegrade (Hassena, 2016). They are also resistant to aerobic degradation and under anaerobic conditions they can be reduced to potentially carcinogenic aromatic amines (Sun et al., 2002). Highly discharged of synthetic dyes into environment without proper wastewater treatment can cause serious water pollution as the effluents contain toxic organic chemicals and heavy metal ions (Wu, 2017). These dyes are also highly soluble, and resistant to degradation by organisms. Consequently, their removal from wastewater remains a difficult but necessary task.

The physico-chemical treatment methods such as chemical oxidation, precipitation and coagulation of the pollutants, reverse osmosis are the common treatment methods, but they are less effective at commercial scale due to the high cost and complexity than adsorption process (Lemeyonouin et al., 2018). Biological process also used to decolorize effluents from textile industries, but it isn't always effective in removing colors due to its low biodegradability of textile dyes. So, tertiary treatments are needed to decolorize dyes before discharge to the environment (Wu & Kuo, 2015).

Advanced oxidation process (AOPs) is the modern and effective treatment technology among other technologies since it can degrade a wide variety of organic compounds via oxidation by hydroxyl radicals. From AOPs photocatalysis by nano scaled TiO_2 particles combined with UV light have attracted a great deal of attentions in waste water treatment that contains dyes and heavy metals, due to their high photocatalytic degradation (PCD) rate. But the recovery and recycling difficulties restricted the utilization of finer TiO_2 particles (F. Li et al., 2008). However, the powder Nano-structured titanium dioxide catalytic efficiency increases when the particle size is too fine. Also, the fine powder is susceptible to aggregation after treatment and difficult to separation, this may require additional cost of separation (Divya et al., 2009).

For simultaneous removal of heavy metals and dyes from the waste waters, several researchers have coated photocatalysts (TiO_2) onto a variety of surfaces like, modified fly ash diatomite, bentonite and clay material is a well-known approach followed to overcome the above drawbacks (Lemeyonouin & Guillaume, 2018). The ideal features of clay including high permeability, cation exchange capability, catalysis, adsorption, large surface area and swelling

ability of clay minerals makes them useful for protecting and reclaiming important environmental resources such as water and land (Asamoah et al., 2018).

In this work a composite heterogeneous photocatalytic system which is titanium dioxide (TiO_2) immobilized with bentonite has been used to perform the oxidation of the water soluble azo dye methyl orange (MO). This dye was selected as a model on the basis of its industrial consumption, water solubility, and toxicity. The composite photocatalyst has dual application during waste water treatment such as adsorption and photocatalytic degradation (Yang et al., 2015).

1.2. Statement of the problem

Increasing demand and shortage of clean water sources due to the rapid development of industrialization, population growth and long term droughts have become a major concern in worldwide. Ethiopia is often referred as a water tower of Africa as many large rivers originate in the Ethiopian highlands and flow to the surrounding countries. However, the country does not reach to the optimum level of providing the access to clean water due to population increase, natural disasters and water pollution.

Currently in Ethiopia discharge of untreated sewage into water and the environment is a common practice which leads to health and economic risks, environmental degradation and disruption of ecological integrity. Dye effluents are usually discharged from different industries such as textile, leather, plastics, cosmetics and printing. So, the presence of dye effluents in water causes series damage to the aquatic animals as well as human beings by mutagenic and carcinogenic effects. As a result, these effluents must be treated at the source before discharged to the environment. Commonly conventional treatment technologies such as, biological and physical methods were used to treat wastewater that contains dye effluents. But the conventional treatment technologies are inefficient due to stable and non-biodegradable nature of dyes. Also conventional treatment technologies are causes of secondary pollution due to incomplete degradation of organic pollutants.

Recently, advanced oxidation processes (AOPs) were used as effective and efficient waste treatment technology. A photocatalysis titanium dioxide supported with UV light was a kind of advanced oxidation process commonly used treatment technology due to, its high oxidizing

properties, physicochemical stability, nontoxic, relatively cheap and resistant to many chemicals (acids, bases and solvents) (Subramani et al., 2007). But there are some drawbacks associated with titanium dioxide (TiO_2) photocatalyst such as promoted only by UV light (wavelength $\lambda<385nm$) , inefficient in natural sunlight, difficult to recycle and recover, the suspension phase during catalytic oxidation is susceptible to agglomeration and difficult for separation.

In order to overcome these problems supporting the photocatalyst titanium dioxide (TiO_2) with porous material is a well-known approach. The combination of photocatalytic properties of TiO_2 and adsorption ability of bentonite composite is a kind of advanced oxidation process used for the complete mineralization of non-biodegradable organic pollutants.

1.3. Objectives

1.3.1. General objective

The general objective of this research is developing and application of composite photocatalyst titanium dioxide (TiO_2) supported bentonite for organic pollutant removal from waste water by taking methyl orange as a model pollutant

1.3.2. Specific objectives

- ✓ To synthesis of the composite photocatalyst (TiO_2/Bentonite) using impregnation process
- ✓ To characterize the raw bentonite, titanium dioxide (TiO_2) and the composite photocatalyst (TiO_2/Bentonite).
- ✓ To conduct a photocatalytic experiment and determine the efficiency of the composite photocatalyst.
- ✓ To analyze the effect of calcination temperature, calcination time and titanium dioxide to bentonite ratio on the dye removal efficiency of composite catalyst.
- ✓ To select the optimum synthesis parameters titanium dioxide-bentontite ratio, calcination temperature, calcination time and
- ✓ To analyze the impacts of dye concentration, UV irradiation time and catalyst dose on the efficiency of the optimum composite photocatalyst.
- ✓ To analyze and select the best adsorption isotherm model.

1.4. Significance of the study

Discharging dye effluents from different industries causes series environmental problem. Therefore, removal of dyes from wastewater using advanced oxidation process is necessary to overcome their health and environmental risks. This study can ensure the alternative method to remove dyes and also to show TiO_2 supported bentonite composite is efficient, environmentally friendly and economically feasible. This study should be significant in the sense it will:

- ✓ Create understanding on photocatalysis which are cheap, non-toxic, stable, non-hazardous, biologically and chemically inert, recyclable and insoluble under most ambient conditions.
- ✓ Provide economically feasible bentonite supported TiO_2 catalyst
- ✓ Provide useful knowledge on parameters which have impact on the performance of composite.
- ✓ Provide environmentally green treatment technology which avoids secondary pollution generation.
- ✓ Creates understanding how photocatalysis is efficient for dye removal from wastewater.
- ✓ Creates awareness on the use of local bentonite as TiO_2 support for the development of composite which is efficient for dye removal.

Chapter 2

LITERATURE REVIEW

2.1. Dyes and water pollution

Water pollution has become a subject of global environmental concern in recent years (Hadjltaief et al., 2015). Water pollution occurs when large percentage of waste products discharged directly into water sources without treatment especially in developing countries where sewage treatment is currently low (Ademe & Alemayehu, 2014). Waste-water generally contains high levels of organic material, numerous pathogenic microorganisms, as well as nutrients and toxic compounds (Reddy et al., 2011). Organic chemicals which may be present as pollutants in wastewater effluents from industrial or domestic sources must be removed or destroyed before the water can be discharged into the environment (Shan et al., 2010).

The presence of organic compounds in water causes the depletion of dissolved oxygen (DO). This also poses environmental problems since it reduces the population of beneficial microorganisms that can naturally degrade organic pollutants (Padhi, 2012). The depletion of DO results increase the amount of chemical oxygen demand (COD) and biological oxygen demand (BOD) which is the amount of oxygen required to completely oxidize the organic pollutants in water chemically and biologically respectively (Segneanu et al., 2013).

The textile industry is one of the oldest industrial sectors in the world which consume large volume of water and chemicals for wet processing of textiles (Environment, n.d.). The effluents from textile units have various types and qualities of wastewater. The wastewater from printing and dying units in a textile plant are often rich in color, containing residues of coloring agents and chemicals, and needs appropriate treatment (Segneanu et al., 2013).

2.2. Dyes

Dyes, generated by various manufacture industries such as dyestuffs, textile, paper, food, cosmetics, leather, and plastics, are the most common contaminants in wastewater (Hassaan & Nemr, 2017).

The discharge of coloured waste is highly problematic, firstly due to the toxic nature of some dyes or of their biodegradation products and secondly due to their visual impact because dyes are visible even at low concentrations (Azami et al., 2013). At present, 100,000 different types of dyes are produced of which about 36,000 tons dye/year are consumed by the textile industries. Up to 20 % of the total world production of dyes is lost during the dyeing process and is released in the textile effluents (Reza et al., 2015).

Industrial effluents contain different chemicals especially synthetic dyes which are carcinogenic in nature. Some dyes decompose aerobically and anaerobically resulting in the formation of carcinogenic compounds (Ullah et al., 2012). Disposal of dyes into water streams causes skin allergies, cancer and eye irritation in human beings (E. M. Wu & Kuo, 2015). Different kinds of dyes, mostly are synthetic ones, are commercially available in the markets. Synthetic dyes are classified into several categories: basic or cationic dyes, the direct dyes, the acid dyes, premetallized dyes, sulfur dyes, azoic dyes, vat dyes, collective dyes, and dyes for fabricated fibers(Hadjltaief et al., 2015).

2.2.1. Azo dyes

Textile industries produce large amounts of wastewater containing various dye pollutants and more than 60% of dyes used in these industries are azo dyes (Al-qaradawi & Salman, 2002). Most of these dyes are stable and non-biodegradable and their release into the environment poses a major threat to the surrounding eco systems (Konsowa et al., 2018). Azo dyes, constituting the largest class among the synthetic colorants, are considered as widespread environmental pollutants associated with many important industries, such as textile, food colorants, printing and cosmetic manufacture (Azami et al., 2013). These azo dyes are found to be complex in nature and have been found to show carcinogenic evidences on reductive cleavage. These dyes are capable of altering the physical and chemical properties of soil, deteriorating water bodies and causing harm to the flora and fauna in the environment (Hassaan & Nemr, 2017).

2.2.2. Basic dyes

Basic dyes are water-soluble cationic dyes applied to substrate with anionic character where electrostatic attractions are formed. Some examples of basic dyes are Methylene Blue,

Rhodamine B, Crystal Violet, Congo red, Methyl Orange, etc. Some of these synthetic dyes have been known to have potential hazards to human health, and their effect is mainly carcinogenic, mutagenic and teratogenicity (Laysandra, Winda, et al., 2017).

2.2.3. Methyl orange

Methyl Orange is a water-soluble azo dye, which is widely used in the textile, printing, paper manufacturing, pharmaceutical, food industries and also in research laboratories. In the Analytical Chemistry Laboratories it is mainly used as an acid base indicator due to its ability to function as weak acid as the aqueous solution of the dye has a pH value of approximately 6.5 (5 g/L, H_2O, 20^oC) (Mittal et al., 2007). Methyl Orange whose chemical name Sodium p-dimethyl amino azo benzene sulphonate ($C_{14}H_{14}N_3NaO_3S$) which has a molecular weight of 327.33g/mole with molecular structure shown below.

Table 2.1: Molecular structure and properties of methyl orange

Alternative name	Heliannthine
Abrevation	MO
Molecular structure	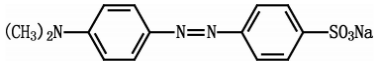
Emperical formula	$C_{14}H_{14}N_3NaO_3S$
Molar mass	327.33 g/mol
Colour	Orange
λ_{max}	465 nm

2.3. Waste water treatment

Waste water treatment is a process of making water suitable for its application or returning its natural state (Tulip, 2017). Industrial water treatment is important, since industrial effluents are often discharged straight into nature and the contaminants may end up into fresh water sources such as rivers, lakes and ground water. In rural areas, people are consuming these waters without any purification (Pirilä, 2015).

Pollutants in waste water effluent from industrial manufacturers and normal households, and in landfill leachates. They can be found in ground water wells and surface waters. In all cases they have to be removed to protect our water resources or to achieve drinking water quality (Turkar et al., 2011). The principal purposes of water treatment is to remove water contaminants like, solids, pathogens, bacteria, algae, inorganic and organic compounds from water (Laysandra, Winda, et al., 2017).

2.3.1. Overview of recent water treatment technologies

In recent times considerable attention has focused on the safety and efficiency of water treatment technology. A wide range of water treatment methodologies has been developed for the removal of synthetic dyes from waters and wastewaters to decrease their impact on the environment (Konstantinou & Albanis, 2004). Many dyes and other organic contaminants are tough to degrade in nature and require more advanced techniques for their removal. Currently a number of techniques and process including physical, chemical and biological methods have been studied to treat dyes in waste water (Tulip, 2017).

Adsorption and photocatalysis have been considered as effective approaches for dye removal. The adsorption is a nondestructive process, by which the contaminants can be transferred from wastewater to adsorbent such as clay bentonite and activated carbon (AC) (Xing et al., 2016). However, the adsorption efficiency of the adsorbents after regeneration is greatly reduced. Also Conventional water treatment technologies such as solvent extraction, activated carbon adsorption, and chemical treatment process [such as oxidation by ozone (O_3)] often produce hazardous byproducts and generate large amount of solid wastes, which require costly disposal or regeneration method (Reza et al., 2015).

According to Krasner, (2009) conventional water treatment methods are susceptible to the generation of secondary pollutants when discharged into the ecosystem after treatment. Also some of conventional water treatment processes such as ozonolysis and chlorination create disinfection by-products (DBP) such as bromate and trihalomethanes respectively, which have mutagenic and carcinogenic health risks to humans (Verne, 2009).

Table 2.2: Advantages and disadvantages of some conventional treatment technologies

Treatment process		Advantages	Disadvantages
Chemical methods	Coagulation Flocculation Precipitation	✓ Low capital cost and short detention time. ✓ Relatively good elimination efficiency.	✓ Agglomerates & treatment only on selected operating conditions.
Biological methods	Aerobic process	✓ Partial or complete degradation for all dye classes	✓ Costly treatment method
	Anaerobic process	✓ Resistant to wide range of complex coloured compounds	✓ Long adaptation phase
Physical treatments	Membrane filtration	✓ Removes all dye types, recovery ✓ Reuse of chemicals and water.	✓ Has high operation cost ✓ Concentrated sludge production
	Activated carbon	✓ Good elimination efficiency of wide variety of dyes. ✓ Economically attractive	✓ Susceptible to excessive sludge production

Some organic pollutants are classified as bio-recalcitrant, are not biodegradable which can't be removed by those conventional treatment techniques. In this case in comparison among adsorption, advanced oxidation processes (AOPs) may become the most widely used water treatment technologies for organic pollutants not treatable by conventional techniques (A. E. Segneanu, C. Orbeci, C. Lazau, P. Sfirloaga, P. Vlazan, C. Bandas, 2013). Among the various AOPs, semiconductor mediated photocatalysis has been accorded great significance in recent times due to its potential to mineralize a wide range of recalcitrant organic pollutants at ambient temperature and pressures into harmless substances (Shan et al., 2010).

2.3.2. Adsorption

Adsorption is the separation of a substance from one phase accompanied by its accumulation or concentration at the surface of another. It is the process that takes place when a liquid or gas known as the adsorbate accumulates on the surface of a solid adsorbent and forming a molecular film (Anocomposites et al., 2017). Adsorption technology which categorized under physical techniques are one of the promising treatment options for pollutant removal due to its efficiency, simplicity, inexpensive and unaffected by toxicity (Yahya et al., 2018). When solely utilized, this method is unable to completely eliminate or destroy the pollutants, but rather concentrates the pollutants through absorption and separates it from the system. Different conventional and non-conventional adsorbents, such as activated carbon, zeolite and clays have been manufactured for the uptake of dyes (Salem & Saghapour, 2016).

Clay minerals act as natural adsorbents in the removal of contaminants from water passing through the soil (Salem & Saghapour, 2016). Also natural and synthetic clays are receiving increasing attention as supports of TiO_2 based photocatalysts for air and water remediation due to its large surface area used for reversible and irreversible adsorption of organic pollutants (Kibanova et al., 2009).

Clays are layered minerals with space between the layers where they can adsorb positive and negative ions as well as water molecules (Sobota, 2016). Although clays are very useful for many applications, they have one main disadvantage i.e. lack of permanent porosity. To overcome this problem, researchers are looking for a way to prop and support the clay layers with molecular pillars. Most of the clays can swell and thus increase the space between their layers to accommodate the adsorbed water and ionic species. These clays are employed in the pillaring process (Karimi & Salem, 2011).

Ultra-fine TiO_2 powders have large specific surface area and has good photocatalytic efficiency, but due to their easily agglomeration into larger particles, an adverse effect on their catalytic performance has been observed (Laysandra, Winda, et al., 2017). It has been shown that the recovery of pure TiO_2 powders from aqueous systems is difficult. Embedding TiO_2 nanoparticles in clay matrices is expected to improve the photocatalytic performance by enhancing VOC

retention through adsorption in clay pores and which is the best solution to overcome the above problems (Kibanova et al., 2009).

In addition synthesis of TiO_2 nanoparticles embedded in the structure of porous clays avoids the formation of macroscopic aggregates of photoactive particles that may lead to reduced efficiency. Furthermore, clays are stable supports that protect the TiO_2 particles from erosion or washing, and are inexpensive, nontoxic materials (Yahya et al., 2018). Clay also have been identified as a good adsorbent due to its wide surface area, stability factor in term of chemical and physical, phyllosilicates material and high cation exchange capacity (Lemeyonouin & Guillaume, 2018).

2.4. Bentonite

Bentonite is an aluminum phyllosilicate generated frequently from the alteration of volcanic ash, consisting predominantly of smectite minerals, mostly montmorillonite (MMT) (80-90 % by weight). Montmorillonite is the most studied phyllosilicate as a matrix for the growth of TiO_2 nanoparticles, as is evident from the number of research works on this subject (Kočí et al., 2011).

The most common impurities in bentonite clay are quartz, calcite, feldspar, cristobalite, beotite, kaolinite, mica and organic matter while hydrated iron oxide, ferrous carbonate and pyrite are being the minor impurities depending on the nature of their genesis (Abdullahi & Audu, 2017). The smectite series, according to the position of its metal ions, can be categorized into montmorillonite, saponite and nontronite (montmorillonite belongs to the smectite series).

Table 2.3: Basic description of the constituent mineral of bentonite

Mineral	Chemical formula	Crystal structure
Montmorillonite	$(Na,Ca)_{0.33}(Al,Mg)_2(Si_4O_{10})(OH)_2.nH_2O$	Monoclinic
Quartz	SiO_2	Trigonal
Hematite	Fe_2O_3	Hexagonal
Feldspar	$KAlSi_3O_8$-$NaAlSi_3O_8$-$CaAl_2Si_2O_8$	Triclinic
Muscovite	$KAl_2(Si_3Al)O_{10}(OH)_2$	Monoclinic

2.4.1. Structure of bentonite

Bentonite is primarily a Na-montmorillonite, whose theoretical formula is equal to pyrophyllite [$(OH)_4Si_8Al_4O_{20}$] (Lin et al., 2012). Montmorillonite is a 2:1 layered silicate in Fig. , and its unit layer structure consists of one Al-$O_4(OH)_2$ octahedron sheet between two Si-O tetrahedron sheets. In the octahedral and tetrahedral sheets, Al^{3+} and Si^{4+} can often be partly (or all) replaced by other cations like iron. Montmorillonite has the chemical formula sodium calcium aluminium magnesium silicate hydroxide $(Na,Ca)_{0.33}(Al,Mg)_2(Si_4O_{10})(OH)_2 \cdot nH_2O$.

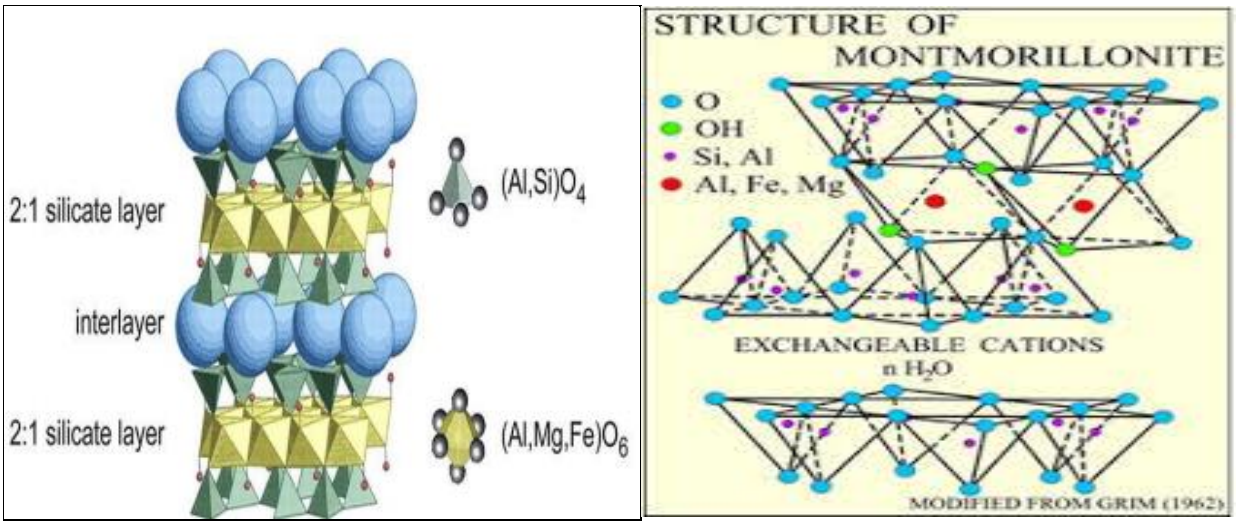

Figure 2.1: A layer structure of bentonite/montmorillonite

Chemical composition of bentonite and fuller's earth is rarely required for industry purposes, usually the physical properties are the most critical. However, in nature chemical composition of bentonite shows considerable variations (SiO_2 is found to vary in range 45-65%, Al_2O_3 17-25% and Fe_2O_3 up to 12%) (Asamoah et al., 2018).

2.4.2. Classification of bentonite

In general, the bentonite is classified into two types. These are Na-bentonite and Ca-bentonite (Abu-jdayil, 2011).

a) Na-bentonite

Na- bentonite has extensive water absorption properties, accompanied by high swelling ability and ability to suspend in water dispersion for long periods of time. This type of bentonite (Na-bentonite) has a single water layer particles containing Na^+ as an exchangeable ion.

b) Ca-bentonite

When calcium lies between the layers, the mineral is distinguished as a calcium montmorillonite (Salem & Saghapour, 2016). Ca-bentonite which don't show swelling properties to any extent when wetted, and don't remain suspended in thin water disperssions. The non-swelling or calcium bentonite has double water layer particles with Ca_2^+ as the exchangeable ion (Sobota, 2016). Ca-bentonite is largely exploited in the treatment of wastewater because of its high removal capacity. This clay has long been widely employed in the production of active powder (Salem & Saghapour, 2016).

2.4.3. Properties of bentonite

The widespread use of bentonite can be attributed to its physical and chemical properties such as small particle size, high porosity, large surface area and high cation exchange capacity make it a strong candidate as an adsorbent for the removal of many pollutants from waste water (Cheng et al., 2012). Bentonite has excellent adsorption capacity due to its swelling ability when immersed in water. The adsorption capacity of bentonite largely depends on the presence of porous structures such as micropores (<2nm), mesopores (2nm<x<50nm) and macropore (>50nm) (Abu-jdayil, 2011).

2.4.4. Application of bentonite

Due to its special properties, bentonite is a versatile material for geotechnical engineering and as well as their demand for different industrial applications such as construction, pharmaceuticals, cosmetics, papers and clarification of edible oil and mineral oils (Salem & Saghapour, 2016). Bentonite has applications in the cosmetic industry as an agent for firming, in products like shampoos, calamine lotions, facial creams and lipsticks. It makes them homogenous and moisturizing, without leaving fatty deposits. This is possible because of the strong colloidal properties of bentonite (Stojiljkovic et al., 2014).

1) Construction and Civil Engineering

Bentonite in civil engineering applications is used traditionally as a thixotropic, support and lubricant agent in diaphragm walls and foundations, in tunneling, in horizontal directional drilling and pipe jacking (Wu & Kuo, 2015). Bentonite, due to its viscosity and plasticity, also is used in Portland cement and mortars.

2) Pharmaceuticals

Bentonite is used as filler in pharmaceuticals, and due to its absorption/adsorption functions, it allows paste formation. Such applications include industrial protective creams, calamine lotion, wet compresses, and ant irritants for eczema. In medicine, Bentonite is used as an antidote in heavy metal poisoning. Personal care products such as mud packs, sunburn paint, baby and face powders, and face creams may all contain bentonite.

3) Paper

Bentonite is crucial to paper making, where it is used in pitch control, i.e. absorption of wood resins that tend to obstruct the machines and to improve the efficiency of conversion of pulp into paper as well as to improve the quality of the paper. Bentonite also offers useful de-inking properties for paper recycling. In addition, acid-activated Bentonite is used as the active component in the manufacture of carbonless copy paper.

4) Environmental Markets

Bentonite's adsorption/absorption properties are very useful for wastewater purification. Common environmental directives recommend low permeability soils, which naturally should contain bentonite, as a sealing material in the construction and rehabilitation of landfills to ensure the protection of groundwater from the pollutants. Bentonite is the active protective layer of geosynthetic clay liners.

2.4.5. Bentonite in Ethiopia

Huge deposits of bentonite occur in the Afar region at several sites (e.g. Warseisa, Ledi, Gewane area, Hararghe) and at Gidicho Island (Lake Abaya) in Sidamo. In the Afar region, the total resources have been estimated at 170,000,000 t of bentonite, which is deposited in Gewane located about 17 km north-east of the town of Gewane. The second largest deposit is Warseisa, situated 1–3 km north of the Dessie-Assab highway between the Badona River and Warseisa.

2.5. Advanced oxidation process (AOPs)

Organic chemicals, which may be present as pollutants in wastewater effluents from industrial sources, must be removed or destroyed before water can be discharged into the environment (Chaker et al., 2016). Most of these organic compounds are toxic and possess a poor biodegradability. Currently available water treatment technologies (adsorption, coagulation) do not resolve this problem in a satisfactory way (Al-qaradawi & Salman, 2002). They simply remove the problem for further environmentally unfriendly treatment elsewhere. As a response, the development of newer eco-friendly methods able to destroy these pollutants has become an imperative task.

Advanced oxidation processes (AOP) is a recently discovered waste water treatment technology which threats organic pollutants by generating hydroxyl radicals which are responsible for organic degradation (Reza et al., 2017). Due to their strong unselective oxidative power the hydroxyl radicals can degrade almost all organic compounds in nontoxic minerals, CO_2 and H_2O as a final product (Yahya et al., 2018a).

2.5.1. Heterogeneous photocatalysis

Heterogeneous photocatalysis is one of the AOPs, and it uses titanium dioxide or other semiconductor materials as a catalysts activated by UV irradiation. Photocatalysis has been studied widely in the degradation of organic compounds in both liquid and gas phase processes (Pirilä, 2015).

Heterogeneous photocatalysis combined with UV is the most effective and efficient waste water treatment technology among AOPs (Rossetto et al., 2010). The photocatalysis process can break down a large variety of organic com- pounds to CO_2, water and nontoxic minerals, as the degradation products. Complete mineralization of the organic substance is the greatest advantage over the conventional techniques of waste treatment (Subramani et al., 2007). These advanced oxidation processes are better than chemical ones however these are much costly (Ullah et al., 2012).

Evolution of a new branch of science known as nano science has completely replaced the previous technologies due to the following reasons.

- Nanomaterials completely mineralize most of organics and are inexpensive.
- Semiconductors remove completely organic matter from polluted water.
- Nanophotocatalyst are non-toxic, non-corrosive and stable chemically and thermally.
- Photocatalyst are easily available, inexpensive and stable to corrosion in the presence of water and chemicals.

The general and detail process of photocatalytic oxidation of organic compounds in water is classified in the following steps (Segneanu et al., 2013).

i. Diffusion of reactants from the bulk liquid through a boundary layer to the solution-catalyst interface (external mass transfer of the reactants in the fluid phase to the surface).
ii. Adsorption of at least one of the reactants to the active surface sites of the catalyst.
iii. Reactions in the adsorbed phase.
iv. Desorption of the product(s).
v. Removal of the products from the interface of the bulk solution.

2.5.2. Types of semiconductors used as a heterogeneous photocatalyst

The energy level of the lower edge of the conduction band of a semiconductor can be considered to be a measure of the reducing power of photo-excited electrons whereas the upper edge of valence band is a measure of oxidation strength of the holes. Band energies of various semiconductors versus the electrochemical potential of hydrogen and oxygen are depicted in Fig. 2.2.

The band gap energy of TiO_2 as shown in Fig. 2.2 is large (>3.0 eV) thus it becomes a good photocatalyst despite its poor catalytic activity towards electron transfer reactions. The large band gap semiconductors prove to be better photocatalysts than low band gap materials. These principles have found extensive applications in the field of environmental chemistry and pollution control (Anandan et al., 2010).

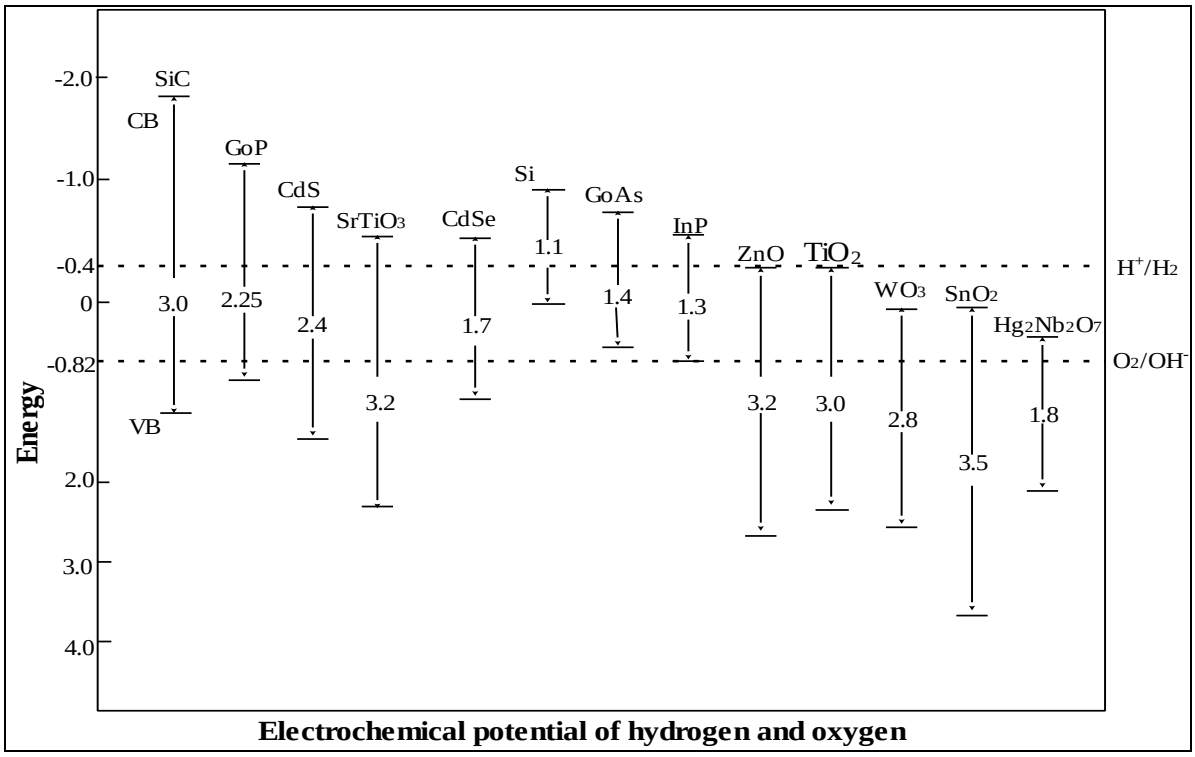

Figure 2.2: Band energy versus electrochemical potential of semiconductors

2.5.3. TiO_2 as a heterogeneous Photocatalysis

Titanium dioxide (TiO_2), also known as titanium (IV) oxide or titania, is the most commonly used catalyst material in photocatalysis (Laysandra, Winda, et al., 2017). It has been reported to be the most promising heterogeneous photocatalyst because of its chemical stability, non-toxic nature, resists most chemicals, inactivation of pathogenic microorganisms, low cost and relatively high efficiency (Subramani et al., 2007). TiO_2 powders such as Degussa P25 have been commercially available for several years. It is to be expected that the photo-activity of semiconductor increases with the decrease of particle size, especially when the crystallite dimension of a semiconductor particle falls below a critical radius of approximately 10nm since, in such a system, the charge carriers appear to behave quantum mechanically. Holes and electrons can be effectively captured by the electrolyte in the solution, which may result in increased rate constant of charge transfer (Sun et al., 2002).

Heterogeneous photocatalytic oxidation (PCO) on semiconductors has been proved to be very promising and effective for degradation of environmental pollutants of polluted water and air, as it has several advantages (Lin et al., 2012).

- ✓ Mild reaction conditions: photocatalysis appears to be active at low or room temperature
- ✓ The final products are innocuous such as H_2O and CO_2, with no secondary pollutants
- ✓ PCO can degrade a broad range of contaminants and also kill bacteria and viruses.

2.5.4. Characteristics of semiconductor titanium dioxide (TiO_2)

TiO_2 comprising approximately 0.62% of the earth crust, is one of the most plentifully distributed element on the earth's surface (Ghosh & Das, 2015). Due to its stability in harsh environments, titanium dioxide (TiO_2) is a ceramic that has the potential to be the material of choice for gas sensors that operate at temperatures above 400^oC (Letters, 2011). This compound is chemically inert in nature, thermally stable and exists mainly in three crystallographic phases namely; anatase, rutile and brookite phases (Khataee & Mansoori, 2011).

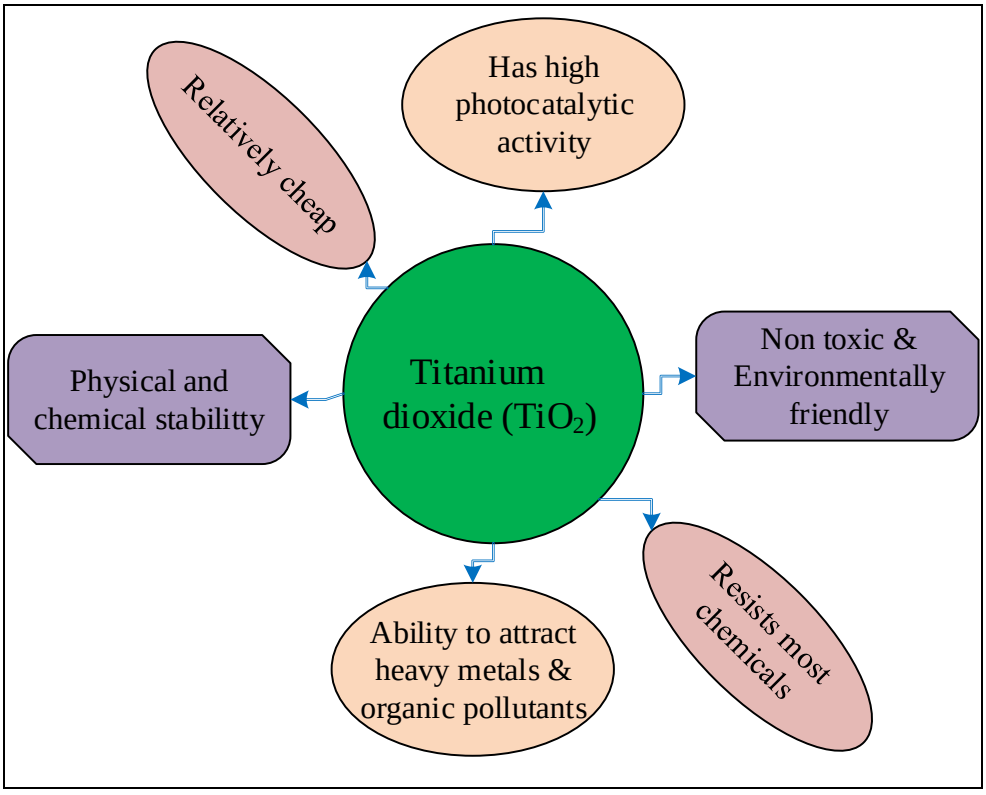

Figure 2.3: General properties of titanium dioxide

2.5.5. The lattice structure of TiO_2

TiO_2 with different crystal structures have different physical properties. In all three polymorphs, a titanium atom is surrounded by six oxygen atoms in an octahedral configuration as shown in the Figure 2-4 below.

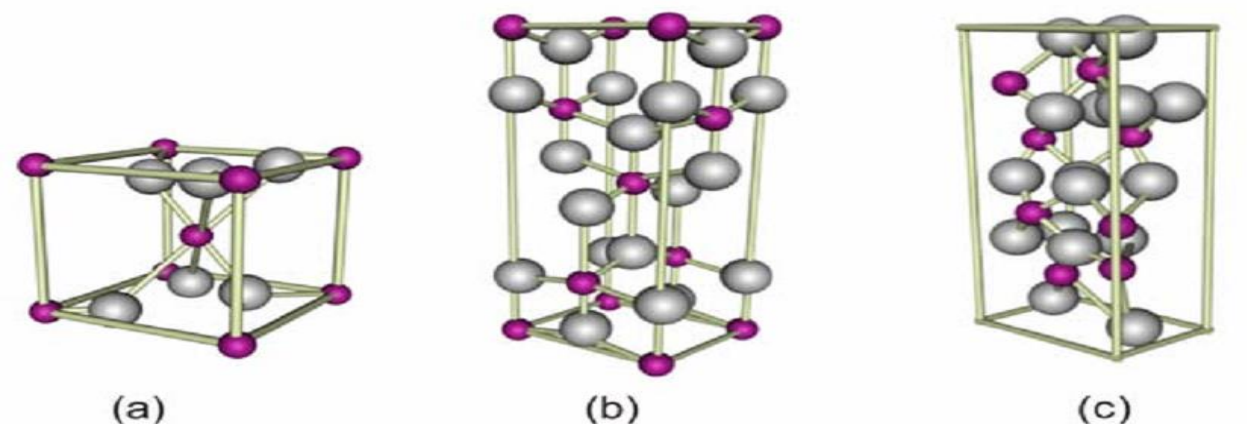

Figure 2.4: Lattice structure of titanium dioxide (a) Anatase, (b) Rutile and (c) Brookite

1) Anatase

Anatase type TiO_2 has a crystalline structure that corresponds to the tetragonal system (with dipyramidal habit) and is used mainly as a photocatalyst under UV irradiation (Letters, 2011). It is thermodynamically less stable than rutile, but it has a higher surface area, and a higher surface density of active sites for adsorption and for catalysis (Bagheri et al., 2014). It is the most common type crystalline structure and its crystalline size is always smaller than the rutile phase. This crystalline phase is thermally metastable phase above 600^oC, experience a phase transition and convert into the rutile phase (Laysandra, Sari, et al., 2017).

The degree of the photocatalytic activity of TiO_2 is proportional to the number of electrons emitted by incident light energy (Fischer et al., 2017). Anatase possesses a lower average effective mass of photo-generated electrons and holes. Therefore, these electrons and holes can migrate with a fast rate from the bulk to the surface, which results in a low recombination rate (Fischer et al., 2017). As a result, the desired hydroxyl and super oxide radicals for the catalytic degradation of organic pollutant can be generated as quickly as possible on the catalyst surface. This makes the photocatalytic efficiency of anatase phase is best compared with the rutile and brookite phase (Anandan et al., 2010). Also its large surface area, high crystallinity, and small

crystal size makes anatase to have high photocatalytic activity (Anocomposites et al., 2017). Generally, the anatase TiO_2 nanoparticles are stabilized by the addition of cations and the phase contains zigzag chains of octahedral molecules linked to each other as shown in the Fig. 2.4 (a)

2) Rutile

Rutile type TiO_2 also consists of linear chains of opposite edge-shared octahedral structure as shown in Fig. 2.4 (b). Rutile phase is the most thermally stable among the three phases and mainly used as white pigment in paint (Letters, 2011).

3) Brookite

Brookite is the third structural form, with an orthorhombic structure, which is rarely utilized, and is of no interest for most applications. It's is also thermally metastable like anatase crystal above 600^oC and experience phase transition into the rutile phase (Fischer et al., 2017).

Table 2.4: properties of crystal phases of TiO2 (anatase, rutile and brookite)

Phase	Refractive index	Density (g/cm^3)	Band gap (eV)	Light wavelength	Crystal structure
Anatase	2.49	3.895	3.26	384	Tetragonal
Rutile	2.903	4.2743	3.02	410	Tetragonal
Brookite	2.583	4.123	2.96	401	Orthorhombic

2.5.6. Photocatalysis process steps

The mechanisms of photocatalytic oxidation of organic compounds at particulate semiconductor substances involve multiple processes. These mechanisms can be categorized in to three major steps involving heterogeneous TiO_2 photocatalysis.

1. Light absorption and generation of electron- hole pairs

When titanium dioxide is irradiated with light that exceeds its band gap energy (3.2eV for anatase) i.e. UV light (wavelength <385nm for anatase), electron-hole pairs are created (Reza et al., 2017). According to the figure shown below electron-hole pairs generated when electron is excited from the valance band (VB) to the conduction band (CB) of the semiconductor, thus creating an electronic vacancy at the valence band edge.

The valence band hole is strongly oxidizing, whereas the conduction band electron is strongly reducing (Shan et al., 2010). This process takes place in a positive region in the VB hole (h^+) and free electron (e^-) in the CB. The valence band hole is strongly oxidizing, whereas the conduction band electron is strongly reducing.

$$TiO_2 \xrightarrow{hv} TiO_2 + e^-(CB) + h^+(VB) \quad (1)$$

2. Migration of electrons and holes to the catalyst surface

The generated charge carriers, i.e., electrons and holes, migrate to the photocatalyst surface. This is affected by factors like the particle size, crystallinity, and the crystal structure of the photocatalyst. However, there is a decrease in the photocatalytic activity of the semiconductor when recombinations of charge carriers occur. After migration, a hole can migrate to the surface; the semiconductor can donate electrons to reduce an electron acceptor. Depending on the charge transfer to the adsorbed species, the semiconductor can act as either an electron donor or an electron acceptor for molecules in the surrounding medium.

3. Oxidation and reduction reaction on the surface of the photocatalyst

Finally, the charge carriers lead to chemical reactions on the surface of the photocatalyst as shown in the Figure (2-5). The holes (h^+) in the valence band diffuse to the surface of the photocatalyst and react with adsorbed water molecules and create hydroxyl radicals. The electrons in the conduction band also interact with water molecules and forms superoxide ($O_2^{\bullet-}$) radicals as shown in the equation (2) and (3) respectively (Anandan et al., 2010).

$$TiO_2(h^+) + H_2O_{ads} \rightarrow TiO_2 + {}^{\cdot}OH + H^+ \quad (2)$$

$$O_2 + e^- \rightarrow O_2^{\cdot-} \quad (3)$$

Then the generated hydroxyl and superoxide radicals can degrade organic pollutants in to carbon dioxide and water on the catalyst surface by oxidation and reduction respectively as shown in equation (4) and (5) (Yahya et al., 2018a).

$${}^{\cdot}OH + MO_{pollutant} \rightarrow H_2O + CO_2 \quad (4)$$

$$O_2^{\cdot-} + MO_{pollutant} \rightarrow H_2O + CO_2 \quad (5)$$

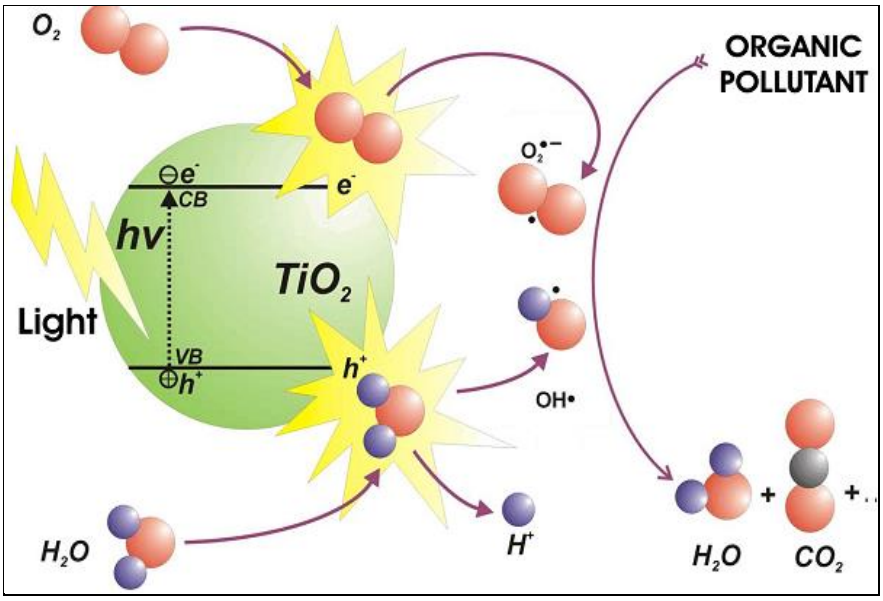

Figure 2.5: Photocatalytic process steps of UV supported TiO_2

The efficiency of TiO_2 is influenced by its crystal structure, particle size, specific surface area and porosity. Ultra-fine powders of TiO_2 show a good catalytic activity. However, agglomeration can take place and this engenders the production of larger particles and resulting in the reduction or even complete loss of catalytic efficiency (Lemeyonouin & Guillaume, 2018).

2.5.7. Methods of improving photocatalytic efficiency of Nano TiO_2

Several methods have been applied to improve the photocatalytic efficiency of TiO_2. A well-known approach for enhancing the photocatalytic efficiency of TiO_2 involves adding a co-adsorbent such as activated carbon (AC), bentonite, graphite and carbon nanotubes (CNTs) (Barka & Assabbane, 2008). The dispersion of TiO_2 particles on clay mineral layers is a potential solution to solve the catalytic and removal efficiency problem. Clay minerals like bentonite supported with TiO_2 show high thermal stability and larger pore sizes that afford better incorporation of the species without diffusion problems, increased specific surface area or increased acidity (Rossetto et al., 2010). The abundance of bentonite in most continents of the country and its low cost make it a strong candidate as an adsorbent for the removal of many pollutants from wastewaters(Cheng et al., 2012).

Another approach for enhancing the photocatalytic efficiency of TiO_2 involves doping with non-metals, such as N, P, B, C, S, F, Cl and Br, has been widely used for the modification of TiO_2 to improve its photocatalytic activity or to extend its light absorption into the visible region (Ullah et al., 2012).

2.6. TiO_2 supported Bentonite Composite photocatalyst

The majority of the charge carriers in titanium dioxide (TiO_2) semiconductors are electrons and holes (Ghosh & Das, 2015). However, these charge carriers show rapid recombination and this is the reason why single component semiconductor (NP) show a comparatively poor photocatalytic activity. Due to this reason industrial treatment of wastewater with various pollutants by photocatalytic oxidation with TiO_2 is uncommon because of the fast recombination rate of the photo-induced electron–hole pair reference. However modified TiO_2 nanoparticles (NP) are considered to be more effective due to different physicochemical properties in comparison to unmodified fine particle analogs (Ghosh & Das, 2015). Several strategies have been employed to modify TiO_2 to reduce recombination rates of photogenerated charge carriers to enhance the optimal functioning of TiO_2. Chemical modification with doing, incorporation of foreign atoms in the titanium dioxide (TiO_2) crystal structure is one of the wellknown strategies in order to synthesize visible-lightactive TiO_2 photocatalyst (Kebede Kassahun et al., 2017).

Several reaserches have pointed out; modifying the nano particle TiO_2 with clay supports is one of the best options to facilitate visible light absorption as well as to improve electron- hole pair recombination reference. The photocatalytic usually TiO_2 supported on materials that are strongly attached to the building blocks are the most promising technologies for depolluting the organic pollutants (Kibanova et al., 2009). Supports should be chemically inert, or participate in the chemical process for facilitating the pollutant elimination. There are certain requirements a good photocatalyst support include (1) to facilitate mass transport to and from the active sites, (2) to increase the effective residence time in the proximity of the photocatalyst and (3) to avoid blocking irradiation from the active sites (Kibanova et al., 2009) check other reference.

A new generation of photocatalysts in composite form in near future is expected to possess high internal efficiency related to separation, and set in contact with external pollutant molecules.

The use of composite materials is a method to improve the activity of a catalyst since composite materials can have higher specific surface areas, improve the reaction conditions, and widen the response range to light (Pirilä, 2015).

Therefore, composite photocatalysts were designed by immobilization of titanium dioxide on the support materials with large surface areas in order to condense diluted pollutants, to separate easily the catalysts from the aqueous solution and to enhance the photocatalytic efficiency (Wang et al., 2009). A few methods that could improve the activity of photocatalysts include surface modifications, band gap modifications, and using composite materials.

The combination of bentonite with TiO_2 was confirmed to be an effective way for separating electron–hole pairs. As a result it can improve the photocatalytic efficiency the photocatalyst (Konsowa et al., 2018). There are various support materials for TiO_2 include, among others, glass, quartz, paper, cement, activated carbon fibers, ceramics, stainless steel, etc (Kibanova et al., 2009). The clay bentonite mineral which contains mainly montmorillonite and quartz impregnated with TiO_2 has high thermal stability and larger pore sizes that afford better incorporation of the species without diffusion problems, increased the specific surface area for better adsorption of pollutants on the its surface (Cherrak et al., 2015). Clay bentonite also consists of an aggregate of flat platelets, has high specific surface area, high plasticity, and non-toxic and expands when wet (Divya et al., 2009). If it used with nano- sized titania makes it easier to separate the titania based photocatalysts. It is therefore, interesting to investigate the photocatalytic activity of composite photocatalysts comprising of titania and bentonite.

2.6.1. Advantages of the composite photocatalyst

Bentonite is a potential and effective catalyst carrier of photocatalyst. Recently, a wide range of studies about preparing bentonite/TiO_2 composite photocatalyst for adsorption-photocatalytic degradation of environmental pollutants have been reported (Lin et al., 2012)**.** The combination of clay support like bentonite with nano structure TiO_2 has many advantages such as,

(1) Adsorbent can absorb the pollutants to increase the pollutants concentration around TiO_2 photocatalyst, thus it can improve the photocatalytic efficiency.
(2) Photocatalytic can degrade the pollutants on the adsorbent, so it can extend the life of adsorbents.

(3) In addition, the adsorbent can absorb harmful intermediates and by-products deriving from the PCO reaction, allowing further degradation on photocatalyst, so as to reduce secondary damage to the environment.

2.6.2. Preparation techniques of bentonite-TiO_2 composite photocatalyst

Various composite photocatalyst preparation techniques have been developed at different time. Sol-gel method and impregnation methods are the common techniques that can be implemented at different industrial process (Santiago et al., 2007). Nevertheless, these methods have some disadvantages for industrial applications. For example, special apparatuses will be needed such as electro-spinning machine (Konsowa et al., 2018). Due to this impregnation method is taken as the most efficient and preferable among others.

1) Sol-gel method

Sol-gel process generally involves the use of inorganic or organic salts such as metal alkoxides or monomers as precursors with solvent to form a colloidal solution (sol) , which is a liquid of solid particles ranging in size from 1nm to 1 micron, that acts as an integrated network (or gel) of either discrete particles or continuous network polymers (H. Li, 2013).

Sol-gel method is preferable for low cost photocatalytic material by coating a support, like a glass plate, with a thin film using the dip-coating method (Hendrix et al., 2015). During the dip-coating method, the support is dipped into a stable sol-gel mixture, and is then slowly pulled out of the mixture so that a thin layer of the mixture is adsorbed to the surface.

2) Impregnation method

Impregnation is a commonly used method in supported catalyst preparation. Impregnated catalysts are usually obtained from preformed supports by impregnation with the active phase. In such preparation methods, the calcination step, which is essential in order to get the photoactive anatase phase, might reduce the surface area of the inert component (support) (Paz, 2010).

The impregnation method involves three steps:

- Contacting the support with the impregnating solution for a certain period of time
- Drying the support to remove the imbibed liquid
- Activating the catalyst by calcination, reduction, or another appropriate treatment

Depending on the total amount of solution used, two types of impregnation can be distinguished. These are dry impregnation and wet impregnation.

a) Dry impregnation:

The principle of dry impregnation is that the volume of the precursor solution used in the impregnation is equal to the pore volume of the support, which results in a better distribution of the solute on the support surface (Lemeyonouin & Guillaume, 2018). In principle this method appears to be simple, economic (especially when using solutions of costly active components) and able to give a reproducible metal loading which is however limited by the solubility of the metal precursor.

b) Wet impregnation

The second type of impregnation, called ``wet" or ``soaking", involves the use of an excess of solution with respect to the pore volume of the support. The system is left to age for a certain time under stirring, altered and dried (E. M. Wu & Kuo, 2015).

2.6.3. Parameters affecting the photocatalytic performance the composite photocatalyst

In photocatalysis, in addition to the physical and chemical properties of photocatalysts, the operational parameters also influence the total photocatalytic activity. Parameters such as photocatalyst dosage, type and initial concentration of the target pollutant, ratio of the semiconductor TiO_2 and the clay support, calcination temperature, calcination time and reaction tieme are the main parameters affecting the photocatalytic performance of the photocatalyst.

a. Surface area

In heterogeneous catalysis, reaction takes place at the active surface of the solid catalyst (Khataee & Mansoori, 2011). So, high surface area is desirable for the photocatalytic system for adsorption of pollutants in the vicinity of the photocatalystic active sites. The adsorption capacity can be generally improved by increasing the specific surface area (SSA) and pore volume of catalysts (H. Li, 2013).

b. Calcination temperature

Calcination is a common treatment that can be used to improve the crystallinity and photocatalytic activities of TiO_2 powders. According to (H. Wu et al., 2014) the photocatalytic

oxidation efficiency of carbon doped titanium dioxide composite photocatalyst can be tuned by changing the calcination temperature, therefore the calcination temperature showed a great influence on the activity of the photocatalysts. When the calcination temperatures is too high, TiO_2 powder experiences phase transformations from amorphous to anatase, or from anatase to rutile (You et al., 2005). The crystal sizes of anatase also increase with calcination time. However, it is little affected by the heating rate.

It is reported that calcination above 465^oC has always resulted in the phase transition from anatase to rutile. The phase transition could be connected to the growth of crystal size, which results in a severe reduction in specific surface area. Consequently, this should also influence the overall catalytic performance of metal heterogeneous catalysts (Bagheri et al., 2014). However, this reduction in the surface area is often balanced by the improved crystallinity of the photocatalyst, provided that the temperatures of calcination remain below the anatase to rutile phase transition temperature (Paz, 2010).

c. Catalyst dosage

Generally, decomposition rate increases initially with photocatalyst dosing due to increases in the number of the available surface active sites for adsorption and interfacial charge transfer. Hydroxyl radicals ($^{\cdot}OH$) are increased with the increase in concentration of photocatalyst resulting de-colorization of the dye. Beyond a certain optimum concentration, the solution opacity increases (due to increased light scattering of the photocatalyst particles) causing a reduction of light penetration in the solution and a consequent the photocatalytic performance decreases (Ullah et al., 2012). For all practical purpose, the limit of composite photocatalyst dosage should be preferentially maintained under 2 g/L when photocatalyst particles are dispersed in an aqueous solution of target pollutant (H. Li, 2013).

d. Titanium dioxide to Bentonite ratio

The proportion of the powder titanium dioxide and clay support plays a great role in the photocatalytic and discoloration efficiency. According to (Dhahir, 2013), when the amount of powder titanium dioxide exceeds the support clay material, it affects the surfaces of the adsorbent and this intern reduces adsorption efficiency of the composite photocatalyst.

e. Dye concentration

Advanced oxidation process is functional only in the presence of UV- light as energy source to promote the excitation of electrons from the lower band gap to the highest conduction band. So, efficiency of UV- light is negatively affected by the target pollutant concentration. The effect of initial concentration of dyes on the percentage degradation was studied by (Reza et al., 2015)

At high initial concentration of dye concentration, all surface active sites are occupied. A further increase of dye concentration reduces desorption of intermediate products and thus block the active sites of the composite photocatalyst, which will cause a decrease of the photocatalytic activity. Meanwhile, at low concentration, degradation of dye pollutant increases linearly with pollutant concentration.

2.7. Related researches regarding to TiO_2 supported by porous materials

Recently, many researchers have been using clay materials to support nano TiO_2 in order to improve the photocatalytic and recovery efficiency of TiO_2.

Wang et al., 2009 uses phenol as a model pollutant and investigated that, TiO_2 supported with activated carbon (AC) for the removal of phenol in waste water. In his investigation he concluded that, the composite catalyst TiO_2/AC prepared at calcination temperature of 900^oC consisted mainly rutile phase showed the highest total removal of phenol and the sample calcined at 700^oC consisted both rutile and anatase phase has the highest photoaactivity for phenol degradation.

According to Moradi & Nasrollahpour (2017), activated carbon (AC) was used as a co-adsorbent to TiO_2 for decomposition of methyl green has been investigated. The adsorption of methyl green on the AC followed by transfer to the TiO_2, where they are photocatalytically degraded. The interface between AC and TiO_2 in the solution is essential. Finally, the researcher concluded that, the presence of nonporous AC sorbent behind TiO_2 catalyst have two major advantages.

(1) Slowing of the recombination rate of photogenerated electron-hole pairs due to hetero junctions.

(2) A large surface area which facilitates the adsorption of organic substances because the adsorption rate is apparently slower by 1:2 orders of magnitude than recombination of photogenerated electron-hole pairs.

Cheng et al., (2012) studied on preparation of bentonite supported Nano titanium dioxide photocatalysts for degradation of methyl orange in waste water. According to this study, the bentonite supported nano TiO_2 photocatalysts can be easily separated and recovered from the water treatment system and demonstrate an enhanced adsorption and photocatalytic ability for the removal of organic contaminant.

Also Cherrak, Hadjel, & Benderdouche, (2015) studied the photocatalytic degradation of hydrocarbons with Na-bentonite, TiO_2 and H_2O_2 as oxidant. The authors also examined the catalytic properties of the composites for degradation of phenol in aqueous solution and ethanol and toluene vapor. These pollutants were degraded at higher efficiency than pure TiO_2.

Chapter 3

MATERIALS AND METHODS

3.1. Materials

3.1.1. Material collection and transportation

The raw calcium bentonite used in this study was collected from Afar region located at North East of Ethiopia. Commercial titanium dioxide and methyl orange were purchased from the local chemical supplier. Also methyl orange which used as a model pollutant was purchased from the local chemical suppliers. Raw calcium based bentonite was purified using hydrogen per oxide (H_2O_2) to remove organic pollutants. After the purification process was completed, bentonite was separated from the solution by vacuum filtration. Then, the filtrate was washed repeatedly with distilled water and dried in an oven which was maintained at a temperature of 105^oC for 24 hour. The purified bentonite was pulverized in a hummer mill and sieved using vibration screen to get the desired particle size (100-150µm).

3.1.2. Equipment used

Table 3.1. List of equipment

Equipment	Model	Application
Hammer mill	-	Size reduction (1st)
Vibration screen(sieve)	Retsch, AS200	To sieve the sample
Overhead stirrer	EUROSTAR 40	To mix TiO_2-bentonite mixtures
Drying Oven	Memmert 100-800	To dry the sample
Pestle and mortar	5657 HAAN	Size reduction (2nd)
Muffle furnace	-	To conduct calcination
Analytical balance	EP214C	To weigh sample
Magnetic stirrer	HG-3	For continuous mixing of solutions
UV lamp	-	To supply UV light
Centrifuge	UNIVERSAL320R	To filter the treated solution
UV-Vis spectrophotometer	UVD-3200	To measure absorbance of a sample

3.2. Methods

3.2.1. Synthesis of Bentonite supported titanium dioxide (TiO_2) composite

The bentonite titanium composite photocatalyst was prepared through a impregnation method (Hadjltaief et al., 2015) with certain modification. First, a known amount of titanium dioxide in the ratio of 1:10, 2:10 and 3:10 was mixed with 100ml of distilled water. Subsequently, the corresponding amount of bentonite was added to the mixture and heated at 100^{o}C for 1 hour under continuous stirring using overhead stirrer. Then the slurry was filtered using vacuum filter and dried in oven maintained at a temperature of 90^{o}C for 24 hour. The dried mixture was ground using pestle and mortar and sieved in rotary sieve with a particle size of 100-150µm. Lastly, the produced powder was calcined in a muffle furnace at three different calcination temperatures (400^{o}C, 500^{o}C and 600^{o}C) and three calcination time.

3.2.2. Characterization composite catalyst

After the composite catalyst was synthesized at different parameters, it was characterized. Crystal structure, functional groups, specific surface area and crystal size of the raw bentonite, TiO_2 and composite catalyst were very important parameters and needs to be characterized.

(1) XRD Analysis

The crystal phase compositions of raw bentonite, titanium dioxide and the composite titanium dioxide supported bentonite composite was determined at Addis Ababa University laboratory of Faculty of Natural and computational science, department of chemistry using X-ray diffraction (XRD) measurement with analytical brand Rigaku, Mini Flex600 diffractometer with Cu-Kα radiation (λ=0.15406), accelerating maximum voltage (40 kV) and current (15 mA) at scan rate of 0.02 degree per minute in the range of 2θ = 5^o to 50^o. Also the average crystal size of the raw bentonite and composite catalyst can be determined based XRD plot using Scherer's equation (3.1).

$$D = \frac{k\lambda}{\beta\cos\theta} \quad (3.1)$$

Where, D= crystal size (nm), k is constant (shape factor, about 0.9)), β is full width at half maximum (FWHM, in radian) and θ is peak position obtained from XRD plot

(2) FTIR Analysis

The functional group of raw bentonite and the composite photocatalyst was determined by Spectrum 65FTIR (PerkinElmer) in the range 4000-400 cm^{-1} using KBr pellet at Addis Ababa University faculty of natural and computational science department of chemistry. Different types of chemical bonds and functional groups on the surface of the material and the chemical bonds in a molecule can be determined based on the respective functional group frequency range.

(3) Surface area determination

The specific surface area of the raw bentonite and composite catalyst was determined based on air permeability test (Blain's method) using cement as a standard sample.

$$S = S_S \frac{\sqrt{t}}{\sqrt{t_s}} \quad (3.2)$$

where; S_S, is surface area of cement, t and t_s are the time of the given quantity and the standard (cement) respectively in which air flow through the compacted sample bed. For calibration of the apparatus, a known surface area and the time in which air to flow through the compacted sample bed for standard sample was required. In this study cement was used as a standard sample with time and specific surface area of 377.4m^2/kg and 37.8s respectively. The amount of sample for this test mainly depends on the density of the material. As a result, before performing the test density of the sample was measured indirectly using pycnometer.

3.3. Adsorption and photocatlytic degradation expriment

The photocatalytic activity of the sample was evaluated by the degradation of methyl orange (MO) in aqueous solution. Methyl orange was used as a model pollutant because it was possible to use UV–visible spectroscopy to monitor the degradation under different conditions such as MO concentration, catalyst dose and solar intensity. So first the methyl orange solution at different concentration (1-30mg/L) was prepared by dissolving the requisite quantity of the dye without further purification in distilled water. Consequently, measure the absorbance of the dye solution with UV-spectroscopy and prepare a linear absorbance versus concentration standard curve of MO.

After the standard curve was prepared, the efficient catalyst was selected based on its dye removal efficiency among many composite catalysts synthesized at different parameters.

In selecting the efficient catalyst, calcination temperature, calcination time and ratio of Nano TiO_2 and bentonite ratios were the major factors. Then the photocatalytic experiment was carried out isothermally in an analytical microbial hood that has been modified by UV lamp inside as the light source as shown in Fig.3.1.

Figure 3.1. Photocatalytic experiment in a microbial hood

To measure the discoloration efficiency of the composite photocatalys, first synthetic methyl orange solution was prepared at concentration of 5mg/L .Then 50ml of methyl orange was mixed with 50mg of composite catalyst in continues stirring by magnetic stirrer for 2 hours under UV-light source. Then 14ml of the treated sample in 15ml test tube was centrifuged for 10 minutes to separate the solution from the composite. Absorbance of the sample was measured using UV spectrophotometer at the maximum wavelength of 465nm and the final dye concentration after treatment was determined from absorbance and dye concentration relation from standard curve.

The amount of methyl orange adsorbed by the adsorbent at equilibrium condition was determined by equation (3.3).

$$q_e = \frac{C_O - C_e}{m} * V \qquad (3.3)$$

Where, q_e amount of methyl orange adsorbed at equilibrium (mg/g), C_O and C_e (mg/L) represents concentration of methyl orange in the liquid phase at initial and equilibrium condition respectively. Also m and v represents mass of adsorbent and volume of methyl orange solution respectively.

Also the dye removal efficiency was determined using the following equation.

$$\text{Removal of dyes } (\%) = \left(\frac{C_o - C_t}{C_o}\right) * 100\% \qquad (3.4)$$

where, C_o is initial concentration of dyes in (mg/L) and C_t; is the final dye concentration in (mg/L) after treatment is completed.

3.4. Efficient composite catalyst selection

Efficient composite catalyst among different catalysts synthesized at various synthesis parameters was selected based on its dye removal efficiency. So, in these experiment based on BBD three factors were taken with three levels (calcination temperature (400, 500 and 600^{o}C), calcination time (1, 2 and 3 hour) and TiO_2 to bentonite ratio (0.1, 0.2 and 0.3)) with a total of 15 experimental runs was performed. Then ANOVA results, single and interaction effect of each factors was analyzed. Also numerical optimization to select efficient composite catalyst and optimum parameters was conducted by setting some constraints based on the dye removal efficiency.

Table 3.2: Factors and levels to select the best catalyst

		Factor levels		
Representation	Factors	Low (-1)	Medium (0)	High (+)
A	Calcination Temperature (^{o}C)	400	500	600
B	Calcination time (h)	1	2	3
C	TiO_2 and bentonite ratio	0.1	0.2	0.3

3.4.1. Effect of catalyst dose, dye concentration and UV irradiation time

Based on the selected catalyst using BBD metho the effects of dye concentration, optimum catalyst dose and contact time on methyl orange removal efficiency also analyzed. Also 15 runs were conducted by taking three factors with three respective levels as shown in Table 3.2.

Table 3.3: Factors with levels which affect the photocatalytic performance

	Factor levels		
Factors	Low (-1)	Medium (0)	High (+)
Dye concentration (mg/L)	5	10	15
Catalyst dose (mg/L)	1	1.5	2
Reaction time (h)	2	2.5	3

3.5. Comparison of bentonite and composite performance at different parameters

The dye removal performance of bentonite and composite was measured by varying the values of parameters such as catalyst dose, dye concentration and UV irradiation time independently based on BBD optimization result. To compare the dye removal performance of raw bentonite with the composite, the experiment was conducted with the same procedure except the adsorption experiment was conducted without UV light in case of bentonite.

a) Effect of catalyst dose

The effect of catalyst dose on methyl orange removal performance of bentonite and composite was studied by keeping MO concentration and UV irradiation time at optimum value from BBD. First the MO solution was stirred by magnetic stirrer with different catalyst dose (0.5, 1, 1.5, 2, and 3 g/L) in analytical microbial hood by applying UV-light. Then the sample was centrifuged and its absorbance was measured by UV spectrophotometer. Finally determine the final concentration of MO from concentration and absorbance relation and the dye removal efficiency was determined based on equation (3.4).

b) Effect of MO concentration

Effect of dye concentration on the methyl orange removal efficiency was determined by maintaining catalyst dose and contact time at optimum value by varying the MO concentration (5, 10, 15 20, 30 mg/L). In the same principle after the photocatalytic experiment was completed in the microbial hood with UV light, the sample was centrifuged and its absorbance measured via UV spectrophotometer. Then the final MO concentration and the dye removal efficiency were determined after treatment.

c) Effect of UV irradiation time

Also the effect of contact time on the dye removal efficiency of catalyst was determined by keeping catalyst dosage and MO concentration at optimum value by varyinng UV irradiation time (30, 60, 90, 120, 150, 180 minute). The photocatalytic experiment was conducted in microbial hood with UV light by continuous stirring via magnetic stirrer. After the photocatalytic experiment completed the sample was filtered by centrifuge and its absorbance was determined by UV spectrophotometer. Finally final MO concentration and dye removal efficiency of composite catalyst was measured from the absorbance concentration equation.

3.6. Adsorption isotherm

Adsorption isotherm model are very useful for predicting adsorption capacities and to design an adsorption system to remove methyl orang (MO) dye from effluents. Also adsorption isotherm was useful to establish the most appropriate correlation for the equilibrium curves. In this study, Langmuir and Freundlich isotherms were employed to represent the adsorption data of MO onto TiO_2/bentonite composites in which, the adsorption experiments were carried out in the dark place in the presence of UV light in order to protect the effect of light.

3.6.1. Langmuir isotherm

The Langmuir adsorption model is the commonly used isotherm which used to quantify the amount of adsorbate (MO) adsorbed on an adsorbent (composite) as a function of partial pressure at a given temperature.

$$q_e = q_{max} \frac{K_L C_e}{1+K_L C_e} \quad (3.5)$$

where, q_e amount of dyes adsorbed by the adsorbent at equilibrium (mg/L), C_e equilibrium concentration (mg/L). Whereas, q_{max} (mg/L) and K_L (L/mg) represent Langmuir's constant related to the maximum adsorption capacity and energy of adsorption respectively. The Langmuir equation can be further rearranged in the following linear form.

$$\frac{C_e}{q_e} = \frac{1}{q_{max} K_L} + \frac{C_e}{q_{max}} \quad (3.6)$$

Then plot $\frac{C_e}{q_e}$ versus C_e from the above equation which gave linear equation with slope of $1/q_{max}$ and intercept $1/q_{max}K_L$ this used for the determination of isotherm constants.

3.6.2. Freundlich isotherm

Freundlich isotherm is based on the following empirical equation not physical, chemical or biological principle.

$$q_e = K_F C_e^{\frac{1}{n}} \quad (3.7)$$

where, q_e amount of MO adsorbed per weight of adsorbent (mg/L), c_e equilibrium concentration (mg/L), K_F and n are Freundlich constants that represent the adsorption capacity of the adsorbent

and heterogeneity of the system, respectively. By taking the logarithmic of the above equation the linear equation obtained as follows.

$$\text{Log}\, q_e = \log K_F + \frac{1}{n} * \log C_e \qquad (3.8)$$

Then plotting graph between $\text{Log}\, q_e$ and $\log C_e$ we get a straight line with the slope value equal to 1/n and $\log K_F$ as y-axis intercept. The value of 'n' changes from 0.2 to 0.9 and increases with temperature increase to 1. The value 'k' changes within a wide range depending on the kind of adsorbent and adsorbed substance.

The general experimental framework for synthesis of TiO_2 supported bentonite composite catalyst and photocatalytic degradation experiment summarized in Fig. 3.2.

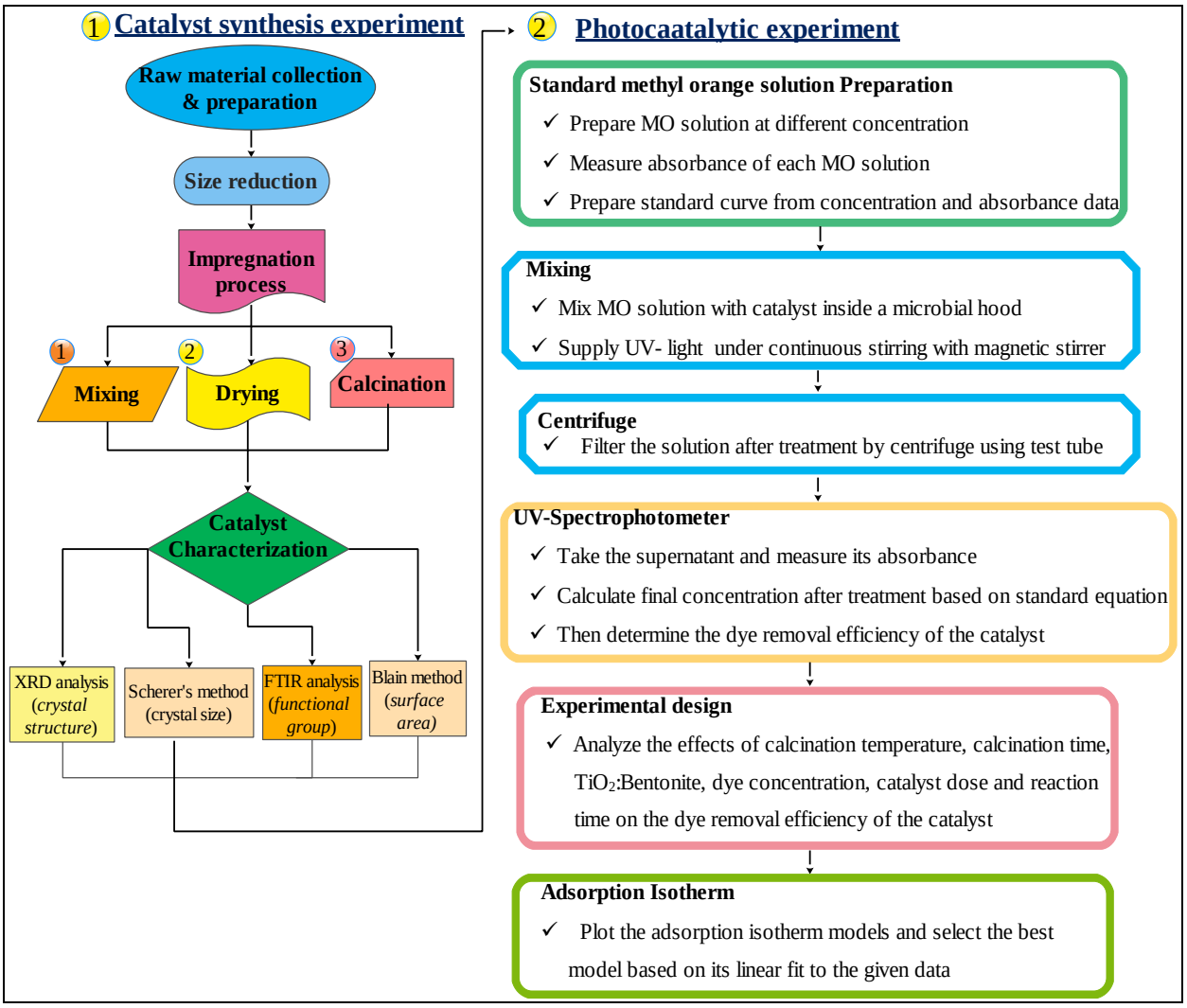

Figure 3.2: Over all experimental frame work

Chapter 4

RESULT AND DISCUSSION

4.1. Characterization of photocatalyst

4.1.1. XRD - analysis result

Figure 4.1 shows the XRD patterns of raw bentonite, powder TiO_2 and TiO_2 supported bentonite composite catalyst synthesized at (calcination temperature (400^oC), calcination time (2h) and TiO_2 to bentonite ratio (0.2). The XRD pattern of anatase and rutile phases were in good agreements with a reference Joint Committee on Powder Diffraction Standards (JCPDS) card No 21- 1272 and 21- 1276 of TiO_2 respectively.

As shown in the XRD pattern of raw bentonite in Fig. 4.1 (a), montmorillonite (Mo), quartz (Q), feldspar (F) and hematite (H) were the most common components. The peaks are located at the diffraction angle of 2θ equal to 17.98^o, 19.91^o, 20.56^o, 21.63^o, 26.74^o, 28.8^o, 34.74^o, 35.88^o and 36.8^o based on International Center for Diffraction Data (ICDD) card No (390381).
The powder anatase titanium dioxide which is the analytical grade consists of anatase and rutile phases with the compositions of 80% anatase and 20% rutile. As shown in the XRD pattern of the powder TiO_2 in the figure 4.1 (b), anatase was dominant peaks observed at diffraction angle of 2θ equal to 25.4^o, 37.95^o and 48.4^o JCPDS card No 21- 1272. Also, rutile was located in the XRD peaks at 2θ equal to 22.93^o, 34.18^o and 43.29^o JCPDS card No 21- 1276.

From the XRD pattern of the composit catalyst shown in Figure 4.1 (c) which was calcinned at 400^oC, anatase phase was observed from the peaks at an angle of 2θ equal to 25.63^o, 38.21^o and 48.40^o according to JCPDS No 21-1272. Rutile phase also observed based on JCPDS No 21-1276 at an angle of 2θ equal to 23.11^o, 34.44^o, 32.00^o, 34.44^o, 38.9^o, and 43.51^o. Also in the composite XRD pattern bentonite components were located at 2θ equal to 20.14^o, 22.06^o, 28.34^o and 35.44^o.

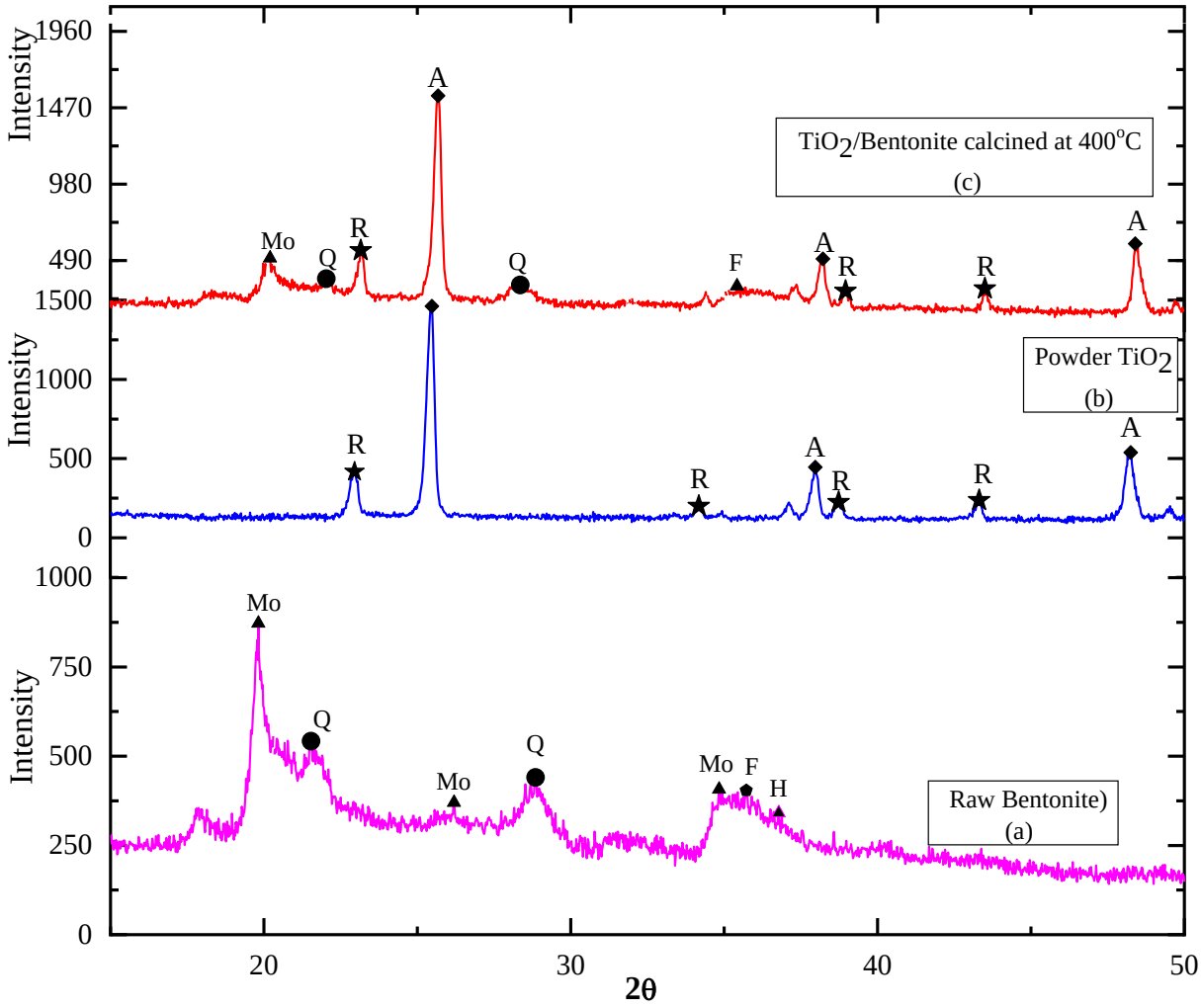

Figure 4.1: XRD plots of (a) raw bentonite, (b) Nano TiO2 and (c) composite

From the XRD patterns of the powder TiO_2 and composite catalyst (TiO_2/Bentonite), the diffraction angle was nearly the same for anatase and rutile phases, but there was additional rutile phase on the composite calcined at 400^oC. This shows that, there was little phase transformation from anatase to rutile at calcination temperature of 400^oC compared with powder TiO_2 shown in Fig. 4.1 (b). As shown in XRD pattern in Fig. 4.1 (c) the intensity of anatase and rutile phase in the composite catalyst was greater than the powder TiO_2. This justified that; calcination can increase the crystallites of the composite which was essential for better removal efficiency.

The XRD reflections corresponding to anatase phase become sharp and narrow with some increment in intensity after calcination at 400^oC in the composite compared with the powder

TiO_2 in Figure 4.1 (c). This can be attributed to the increase of the crystallite size. The average crystal sizes were 24.73nm and 53.43nm for raw bentonite and composite from Appendix B (Table B1 and B2) respectively. These result confirmed that, as the crystal size increases the surface of the composite was reduced. The decrement was mainly due to calcination and due to the impregnation of the Nano TiO_2 on the bentonite surface.

4.1.2. FTIR – analysis result

As shown in Figure 4.2 (a), the infrared absorption band of montmorillonite was observed on bentonite. From these bands, Non- H-bonded hydroxyl group stretches at 3500 to 3700 cm^{-1} which was Al(Mg)-O-H stretching at 3635.2, Si-O-Si stretches in the range of 950 to 1350 cm^{-1} which was 1033.6cm^{-1} in bentonite, Al-OH stretches at 912 cm^{-1}, (Al, Mg)-O stretches at 844.3 cm^{-1}, Si-O bonds stretches at 462.93 cm^{-1} (Silverstein, R.M.; Bassler, G.C.; and Morrill, 1981.).

In the same principle from the FTIR spectra of TiO_2/Bentonite composite as shown in Figure 4.2 (b) the following bands were observed. Hydrogen bonded hydroxyl group (OH) stretches in the frequency range of 3100 to 3600 cm^{-1} in Figure 4.2 (b), H-O-H stretching at 3437.87cm^{-}1, montmorillonite infrared absorption bands located in the composite such as, Al(Mg)-O-H stretches at 3636.23cm-1. Clay particles and TiO2 were observed for TiO_2/Bentonite catalyst was stretched in the range of 1200 to 450 cm^{-1} (Laysandra, Winda, et al., 2017). For instance, in Fig. b for the composite, Si-O-Si stretches at (1041.6 cm^{-1}), (Al, Mg)-O and Si-O stretches at 844.3 cm^{-1} and 462.4 cm^{-1}.

According to Divya et al., (2009) the peak in a composite at 912 cm^{-1} corresponds to the Si-O-Ti bond which suggests that the TiO_2 combine with bentonite by formation of Si-O-Ti chemical bond. And these justified that, powder TiO_2 was impregnated on the adsorbent (bentonite) surface for better photocatalytic purpose.

Additionally, C-H single bond (alkane) functional group stretches in the range of 2960-2850 cm^{-1} and from the fig peaks of 2859.2 cm^{-1} and 2926.93 cm^{-1} were located in TiO_2/bentonite composite catalyst which shows the presence of carbon-hydrogen functional group in the composite catalyst. Carbon-carbon double bond functional group of alkene (C=C) stretches in the range of 1680-1620 cm^{-1}.

So the peaks 1638.3 cm^{-1} and 1640.53 cm^{-1} were located in bentonite and TiO_2/Bentonite composite catalyst respectively and confirmed that the presence of alkene functional group in both bentonite and TiO_2/bentonite composite catalyst. Molecules containing nitro groups (NO_2) also stretches in the frequency range of 1385-1345 cm^{-1} and from FTIR graph the peak at 1381.8 cm^{-1} located in bentonite shows the presence of nitro group in raw bentonite.

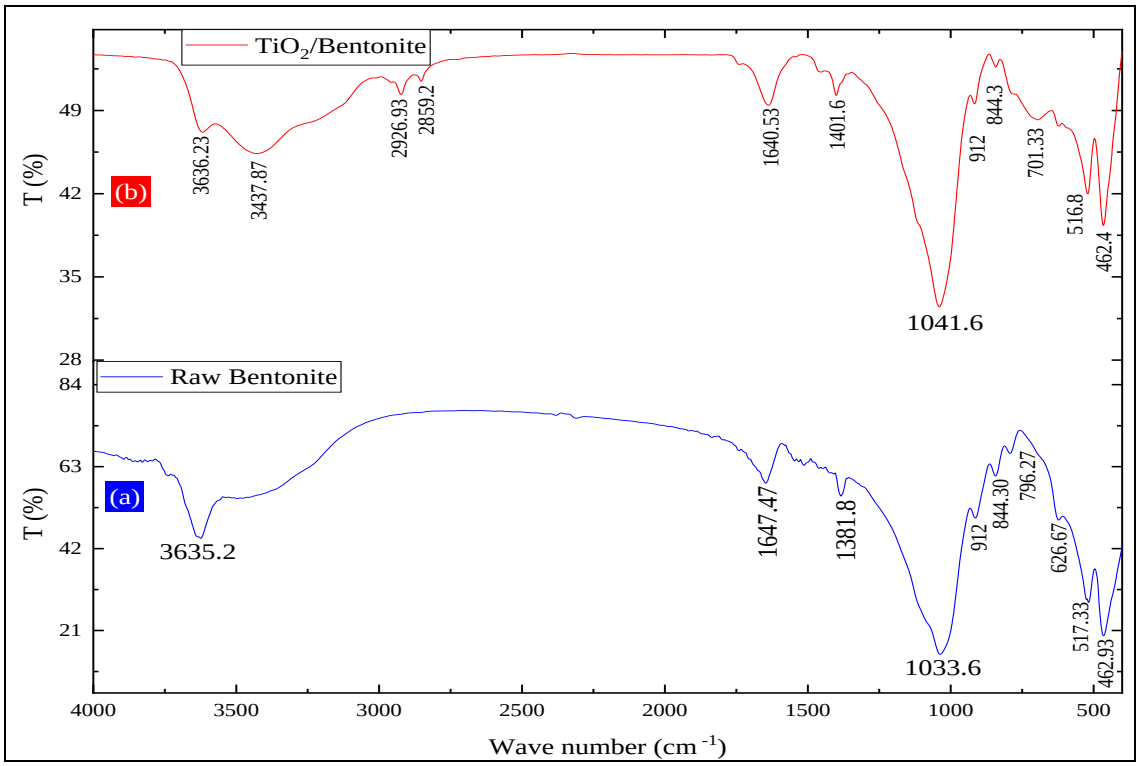

Figure 4.2: FTIR spectra of (a) raw bentonite and (b) TiO_2/bentonite composite

4.1.3. Specific surface area of the raw bentonite and composite catalyst

The specific surface area of bentonite and composite were 148.3m^2/kg and 72.9m^2/kg respectively obtained from equation 3.2. These results confirm that, the surface area of the composite catalyst was smaller than the raw bentonite due to the impregnation of nano TiO_2 on the surface of bentonite.

As a result, the adsorption capacity of the composite catalyst was lowered, but this in turn compensated by the increment of its crystallite of the composite via calcination for better photocatalytic activity (Wu et al., 2014).

4.2. Selecting the efficient catalyst

The efficient catalyst was selected based on its dye removal efficiency calculated based on equation (3.4) summarized in Table 4.1.

Table 4.1: Factors for catalyst synthesis and the corresponding absorbance after treatment

Std order	Factor 1 A:Calcination Temperature (^oC)	Factor 2 B:Calcination time (h)	Factor C:TiO_2:Bentonite ratio	Removal efficiency (%)
1	400.00	1.00	0.20	95.70
2	600.00	1.00	0.20	96.00
3	400.00	3.00	0.20	94.60
4	600.00	3.00	0.20	76.20
5	400.00	2.00	0.10	90.00
6	600.00	2.00	0.10	81.30
7	400.00	2.00	0.30	92.30
8	600.00	2.00	0.30	85.00
9	500.00	1.00	0.10	88.34
10	500.00	3.00	0.10	78.10
11	500.00	1.00	0.30	91.50
12	500.00	3.00	0.30	81.68
13	500.00	2.00	0.20	92.09
14	500.00	2.00	0.20	91.68
15	500.00	2.00	0.20	91.26

4.2.1. Statistical Analysis of the Experimental Result

The analysis of the model with F-value of 301.14 implies the model was highly significant with their corresponding P-value < 0.0001. The ANOVA for the selected response is shown in (Table 4.2). Values of "Prob > F" less than 0.0500 indicate model terms are significant. In this case A, B, C, AB, B^2, C^2 are significant model terms.

Which implies the model was capable to give adquate response inside and outside the given range of the selected model terms.

The "Lack of Fit F-value" of 1.37 implies the Lack of Fit is not significant relative to the pure error. There is a 44.83% chance that a "Lack of Fit F-value" this large could occur due to noise. Non-significant lack of fit is good we want the model to fit.

Table 4.2: Analysis of variance (ANOVA) of the fitted quadratic model

Source	Sum of Squares	Df	Mean Square	F Value	p-value Prob > F	
Model	570.43	9	63.38	301.14	< 0.0001	Significant
A-Calcination Temperature	145.35	1	145.35	690.59	< 0.0001	
B-Calcination time	209.72	1	209.72	996.40	< 0.0001	
C-TiO_2:Bentonite	20.29	1	20.29	96.39	0.0002	
AB	87.42	1	87.42	415.36	< 0.0001	
AC	0.49	1	0.49	2.33	0.1876	
BC	0.044	1	0.044	0.21	0.6663	
A^2	1.31	1	1.31	6.25	0.0546	
B^2	10.03	1	10.03	47.66	0.0010	
C^2	96.92	1	96.92	460.47	< 0.0001	
Residual	1.05	5	0.21			
Lack of Fit	0.71	3	0.24	1.37	0.4483	Not significant
Pure Error	0.34	2	0.17			
Cor Total	571.48	14				

The model adequacy was further investigated using R^2 for one response (dye removal efficiency) which was 0.9982. This implies that, the model was adequate enough to predict the response in the experimental range with 98.82% variability. The Pred R^2 shows that the model equations for dye removal efficiency give good predictions with 97.48% variability. Also the Adj of dye removal efficiency was in reasonable agreement with Pred R^2 values. "Adeq Precision" measures the signal to noise ratio. A ratio greater than 4 is desirable. In this case, the ratio of 52.298 indicates an adequate signal. All the above model adquecy values were for both significant and insignificant model terms and changed when only significant terms were considered (see Table 4.3).

Table 4.3: The model adequacy checking result only for catalyst synthesis

Std. Dev.	0.60	R-Squared	0.9949
Mean	88.38	Adj R-Squared	0.9911
C.V. %	0.68	Pred R-Squared	0.9777
PRESS	12.76	Adeq Precision	47.622

From these results we can conclude that response surface methodology can be potentially used to analyze the relative significance of various impregnation synthesis parameters in the preparation of bentonite supported TiO_2. As demonstrated here Box-Behnken design was properly predict the impregnation parameters with in the selected experimental range as well as outside the given ranges.

Based on the regression analysis the quadratic model equations for one response dye removal efficiency in terms of actual values can be written by considering the significant terms as follows

$$\text{Removal efficiency } (\%) = [65.04417 - (0.015792 * A) + (24.63833 * B) + (201.25833 * C) - (0.046750 * A * B)(1.64833 * B^2) - (512.3333 * C^2)] \quad 4.1$$

Furthermore, the adqueacy of the model was checked by constructing different diagnostic plots for the target response (dye removal efficiency). The normal % probability plots of risiduals for response was normally distributed, as normal plot lies close to the straight line shows the experimental data points were fitted and no deviation of variance in Figure 4.3 (a). Internally studentized residuals plots were constructed to facilitate the satisfactory fit of the developed model see Figure 4.3 (b). The pridicted versus actual plot also shows how the developed models were quite close to the experimental values and lie reasonably close to the straight line and indicates the adquate agreement with real data see Figure 4.3 (c).

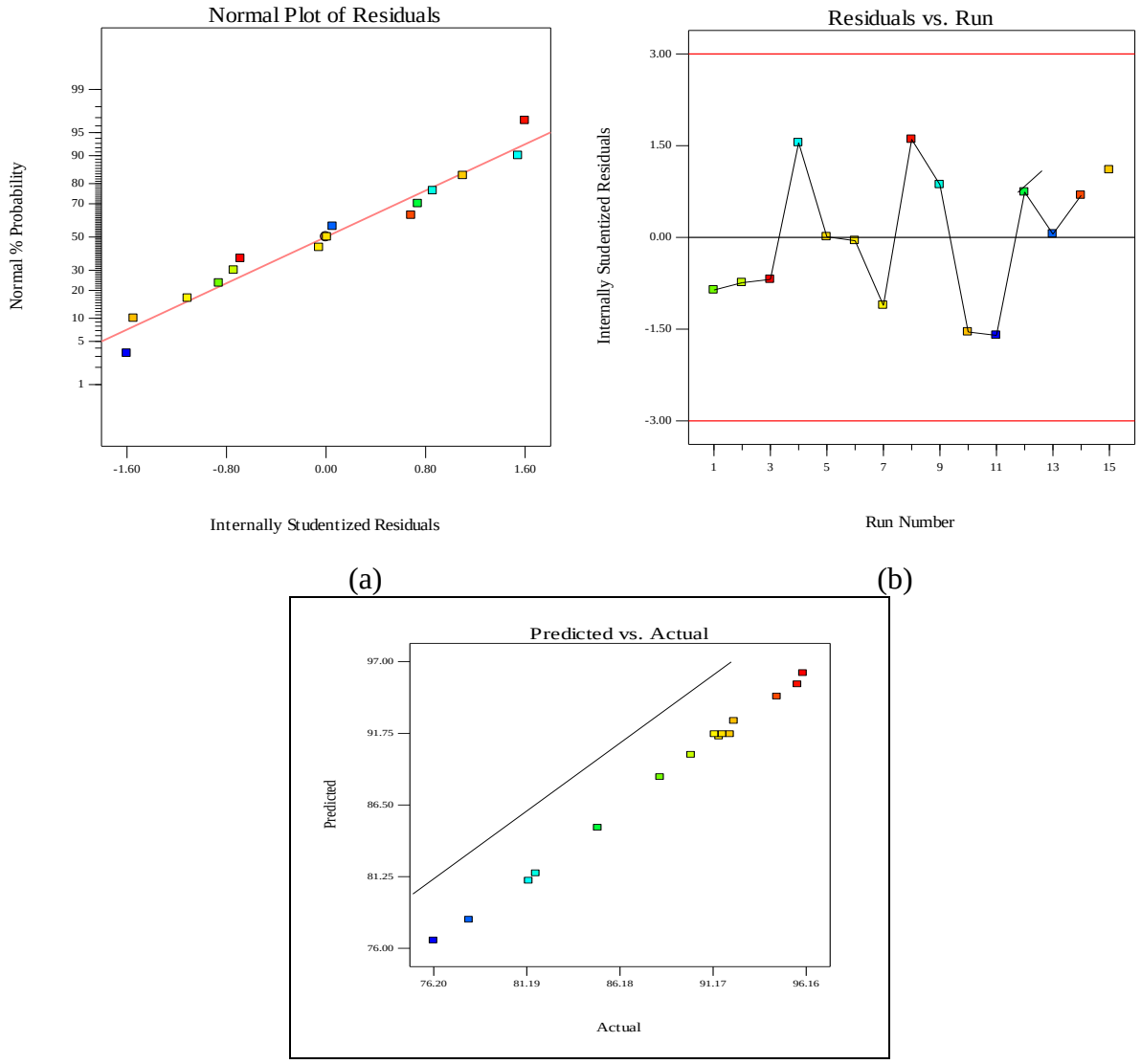

Figure 4.3: Diagnostic plots for the adquecy of the proposed model for dye removal efficiency

4.2.2. The interaction effect of process variables on the target response

a) Effect of calcination temperature and calcination time

According to Fig. 4.4 calcination temperature and calcination time had interaction effect. The variation of one parameter affects the other parameter to have a significant effect on the target response. After interaction point running the process at lower calcination time (1h) gave better removal efficiency by keeping TiO_2- bentonite ratio at optimum value 0.2. Whereas, operating the process at higher calcination time as shown by the red line in Fig. 4.4 gave lower removal

efficiency with increasing calcination temperature. So, to maximize the dye removal efficiency running the process at lower calcination time was preferable.

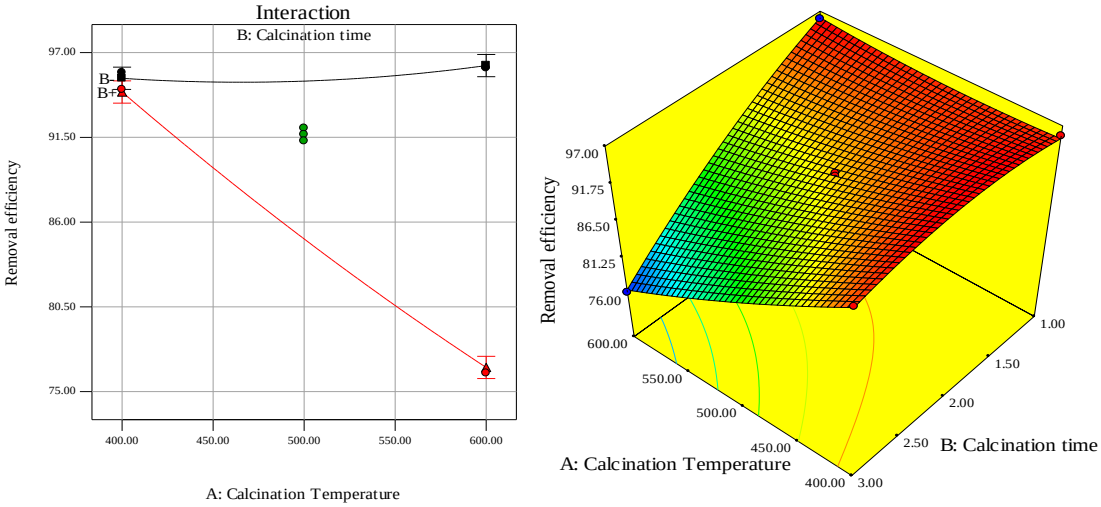

(a) (b)

Figure 4.4: Effect of calcination temperature and calcination time in (a) 2D and (b) 3D

b) Interaction effect of calcination temperature and TiO_2-bentonite

As shown in Figure 4.5, calcination temperature and titanium dioxide to bentonite ratio didn't have any interaction effect on the dye removal efficiency of the composite catalyst. According to Fig. 4.5 running the process at higher TiO_2-bentonite ratio (0.3) by keeping the calcination time at 2h gave better removal efficiency at lower calcination temperature than operating at lower TiO_2-bentonite (0.1).

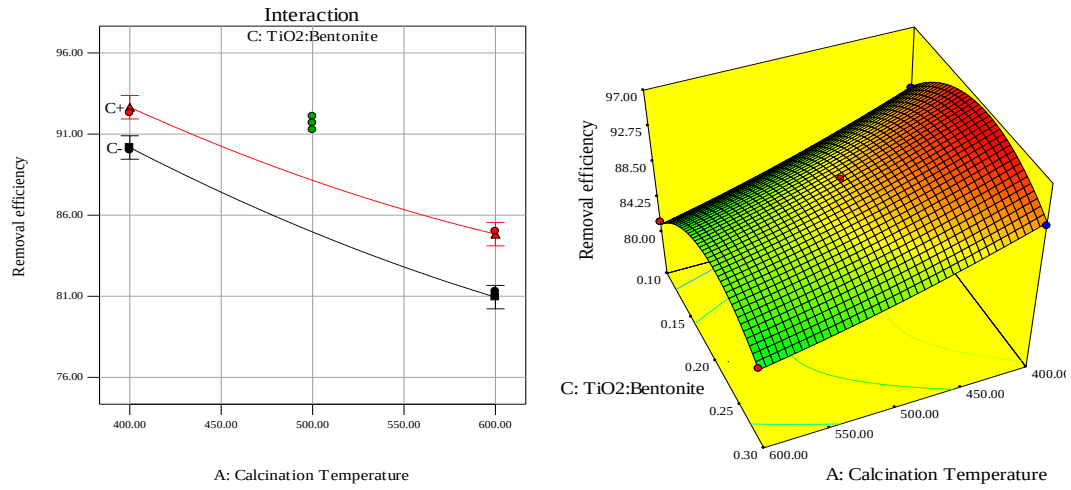

(a) (b)

Figure 4.5 Effect of calcination temperature and TiO_2- bentonite ratio in (a) 2D and (b) 3D

c) Interaction effect of calcination time and TiO_2-Bentonite ratio

Calcination time and TiO_2-bentonite ratio didn't have any interaction effect on the dye removal efficiency of the catalyst as shown in Fig. 4.6 below. From Fig. 4.6 as explained in the red line running the process on higher value of TiO_2-bentonite ratio (0.3) gave higher removal efficiency with lowest calcination time by keeping calcination temperature at optimum value (500 ^oC).

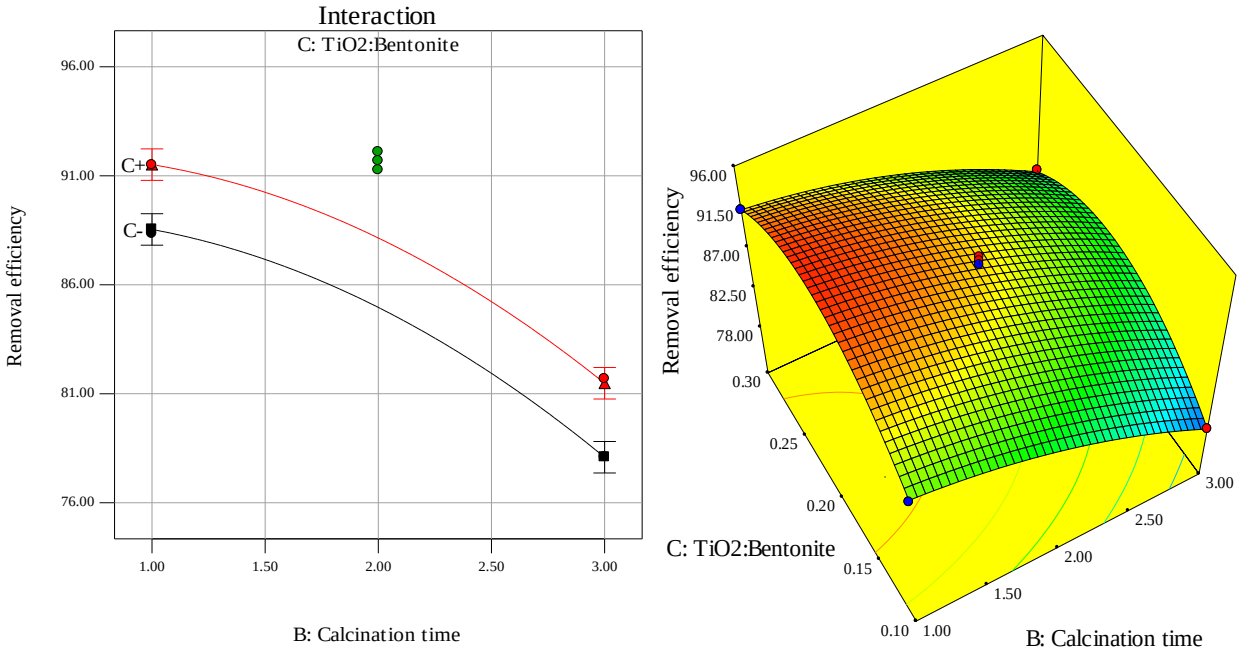

(a) (b)

Figure 4.6: Effect of calcination time and TiO_2-Bentonite ratio in (a) 2D and (b) 3D

4.2.3. Numerical optimization

Lastly the efficient catalyst was selected using numerical optimization for maximum removal efficiency at minimum calcination temperature and for the given range of calcination time and TiO_2-bentonite ratio according to Table 4.4. As a composite calcined beyond 400^OC, the supported bentonite loses its crystallites to amorphous phase which is not good for better photocatalytic activity. As a result the calcination temperature was maintained at minimum value.

Table 4.4: constraints for optimization to select the best catalyst

Name	Goal	Lower Limit	Upper Limit
Calcination Temperature	Minimize	400	600
Calcination time	is target = 2.00	1	3
TiO2:Bentonite	is target = 0.20	0.1	0.3
Removal efficiency	Maximize	76.2	96

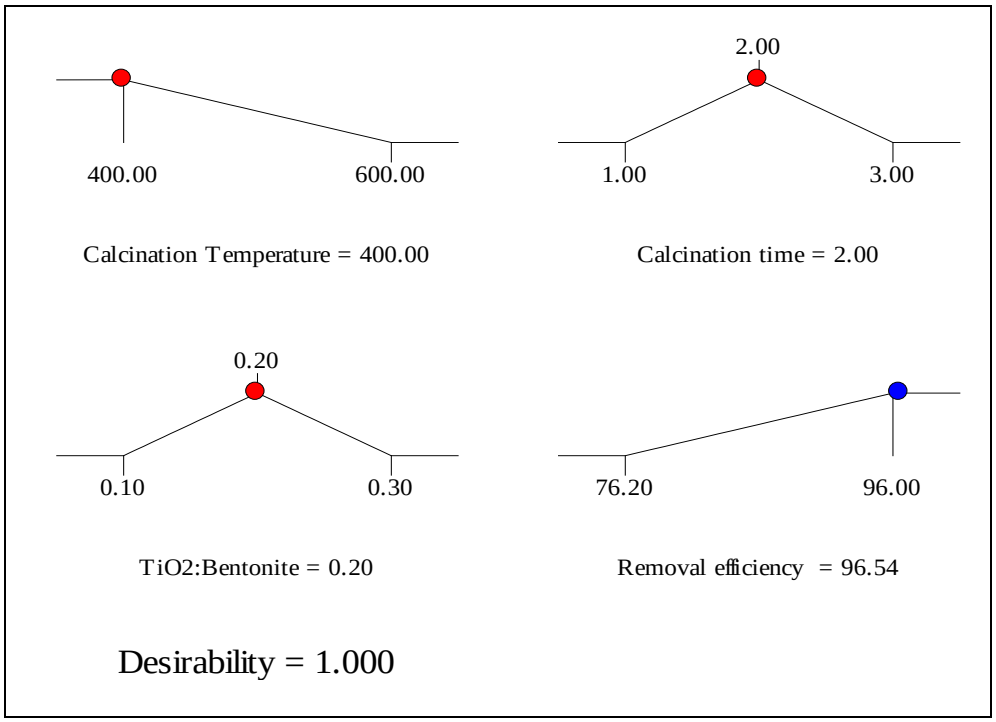

Figure 4.7: Optimization result of the efficient catalyst

According to the numerical optimization result, a calcination temperature of 400^{o}C, calcination time 2hour and TiO_2 to Bentonite ratio of 0.20 was selected with a desirability of 1 to pridict the maximum dye removal efficiency of 96.54%.

To validate the optimum conditions predicted by the model using desirability ramp, triplicate experiments were conducted using the optimized dye removal efficiency process conditions and mean percentage conversion value of 96.27% (96.36%, 97.01% and 96.85%) was obtained and results are closely related with the data obtained from optimization analysis using desirability functions. Therefore, this study shows that impregnation of TiO_2 with clay bentonite enhances MO removal in synthetic solution.

4.3. Effects of MO concentration, catalyst dose and UV irradation time

4.3.1. Stastical analysis of the photocatalytic experimental result

The analysis of the model with F-value of 150.87 implies the model was highly significant with their corresponding P-value < 0.0001. The ANOVA for the selected response is shown in (Table 4.5). Values of "Prob > F" less than 0.0500 indicate model terms are significant. In this case A, B, C, AB, AC, A^2, B^2, C^2 are significant model terms.

Table 4.5: Analysis of variance (ANOVA) result for the photocatalytic experiment

Source	Sum of Squares	df	Mean Square	F Value	p-value Prob > F	
Model	392.67	9	43.63	150.87	< 0.0001	significant
A-Dye concentration	309.78	1	309.78	1071.21	< 0.0001	
B-Catalyst dose	12.99	1	12.99	44.93	0.0011	
C-Reaction time	17.01	1	17.01	58.84	0.0006	
AB	15.28	1	15.28	52.85	0.0008	
AC	3.89	1	3.89	13.47	0.0144	
BC	0.62	1	0.62	2.16	0.2020	
A^2	8.75	1	8.75	30.26	0.0027	
B^2	15.94	1	15.94	55.13	0.0007	
C^2	13.33	1	13.33	46.10	0.0011	
Residual	1.45	5	0.29			
Lack of Fit	1.32	3	0.44	6.94	0.1285	Not significant
Pure Error	0.13	2	0.063			
Cor Total	394.11	14				

The model adequacy was further investigated for significant and insignificant model terms using R^2 for one response (dye removal efficiency) which was 0.9963. This implies that, the model was adequate enough to predict the response in the experimental range with 99.63% variability. The Pred R^2 shows that the model equations for dye removal efficiency give good predictions with 94.57% variability. Also the Adj-R^2 0.9897 of dye removal efficiency was in reasonable agreement with Pred R^2 values. The above model adequacy was changed when considering only the significant model terms (see Table 4.6).

Table 4.6: Model adquecy checking for photocatalytic experiment for experimental result

Std. Dev.	0.59	R-Squared	0.9948
Mean	92.38	Adj R-Squared	0.9878
C.V. %	0.64	Pred R-Squared	0.9580
PRESS	16.56	Adeq Precision	35.994

Further more, the adquacy model can be investigated by plotting some diagnostic adquacy plots such as normal % plot, studentized plot and pridicted versus actual plots were shown in Fig 4.8.

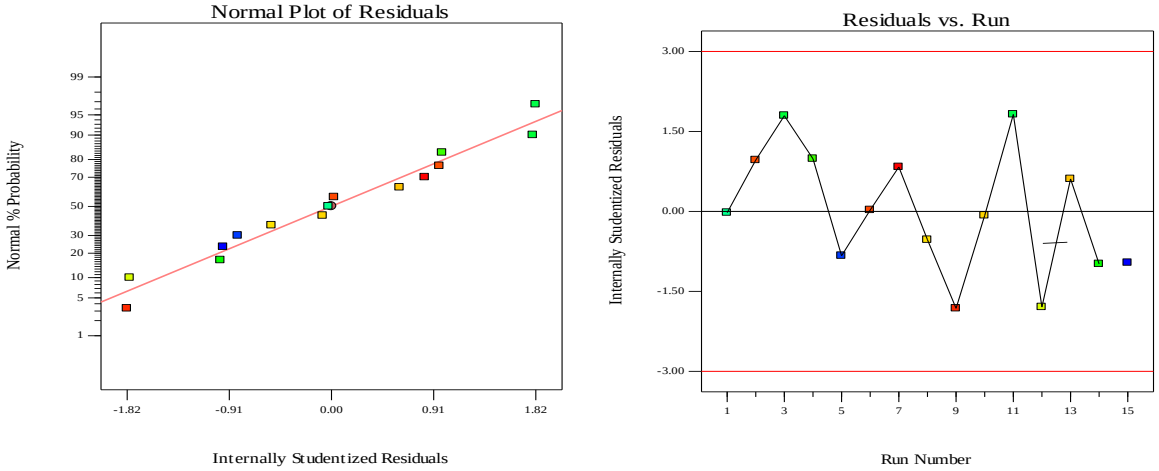

(a) (b)

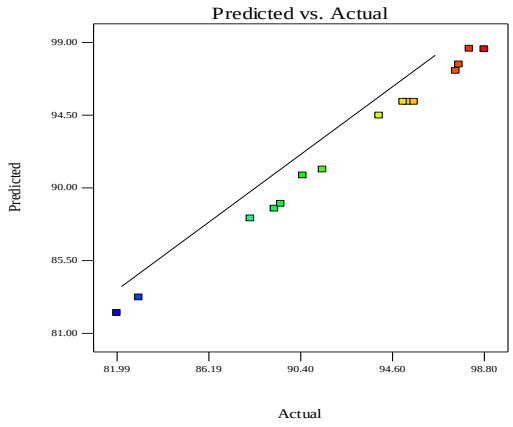

(c)

Figure 4.8: Diagnostic plots for the photocatalystic experiment

Based on the regression analysis the quadratic model equations for one response dye removal efficiency for photocatalytic experiment in terms of actual values can be written by considering only the significant model terms (see equation 4.2)

$$\text{Removal efficieny} = [51.80768 - (2.17244 * A) + (15.71848 * B) + (34.60306 * C) + (0.78186 * A * B) + (0.39469 * A * C) - (0.061582 * A\text{^}2) - (8.31207 * B\text{^}2 - (7.60041 * C\text{^}2)] \quad (4.2)$$

4.3.2. The interaction effect of process variables on photocatalytic performance

1) Interaction of catalyst dose and dye concentration on removal efficiency

According to Figure 4.9 catalyst dose and dye concentration had interaction effect and the variation of one factor has a significant influence on the other factor. As a result, the target response was significantly affected by the interaction of catalyst dose and dye concentration. Before the interaction point operating the process at lower catalyst dose (1) with lowest dye concentration by keeping the UV irradiation time at optimum value (2.5h) gave maximum removal efficiency. Whereas, after the interaction point running the process at higher catalyst dose (2) gave better dye removal efficiency than operating at lower catalyst dose. Therefore, it's better that operating at lower catalyst dose with lower dye concentration was preferable for better dye removal efficiency.

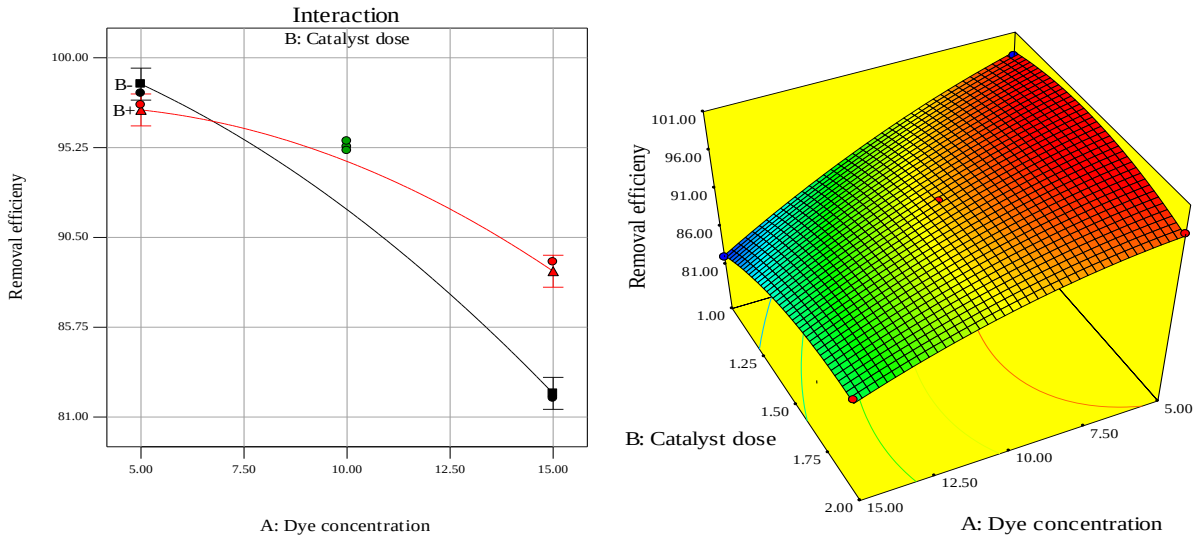

(a) (b)

Figure 4.9: Interaction of catalyst dose and dye concentration in (a) 2D and (b) 3D

2) Interaction of UV irradiation time and dye concentration

Contact time and dye concentration had interaction effect as shown in figure 4.10. According to the figure, operating the process at higher UV irradiation time (3h) with lowest dye concentration

gave better removal efficiency than operating at lower reaction time by keeping the catalyst dose at optimum value (1.5 g/L). Generally the effect of UV irradiation time on the dye removal efficiency significantly influences the dye concentration, which in turn affects the dye removal efficiency.

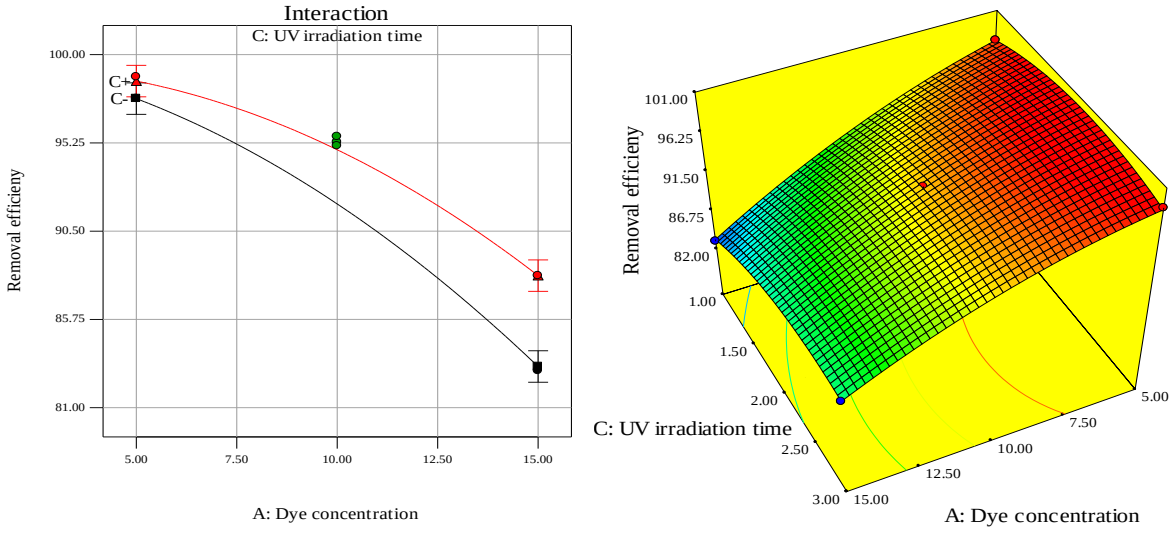

(a) (b)

Figure 4.10: Interaction of UV irradiation time and dye concentration in (a) 2D and (b) 3D

3) Interaction effects of UV irradiation time and catalyst dose

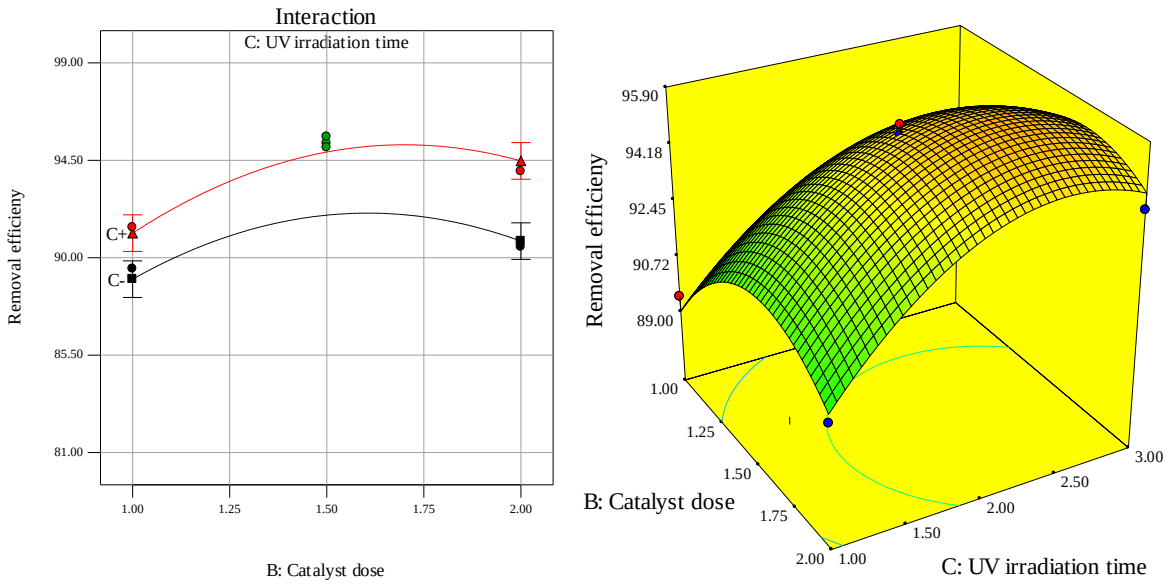

(a) (b)

Figure 4.11: Interaction of contact time and catalyst dose (a) 2D and (b) 3D

As shown in Fig. 4.11, UV irradiation time and catalyst dose didn't have interaction. As a result, the variation of UV irradiation time didn't affect catalyst dose. Simply running the process at higher UV irradiation time (3h) with higher catalyst dose gave better removal efficiency by maintaining the dye concentration at optimum value (10 g/L).

4.3.3. Numerical optimization

The optimum dye concentration, reaction time and catalyst dose were numerically optimized based on dye removal efficiency of the selected catalyst based on the following constraints.

Table 4.7: Constraints for numerical optimization of the photocatalytic experiment

Name	Goal	Lower Limit	Higher Limit
Dye concentration	is target = 10.00	5	15
Catalyst dose	is target = 1.50	1	2
UV irradiation time	maximize	1	3
Removal efficieny	maximize	81.9931	98.8

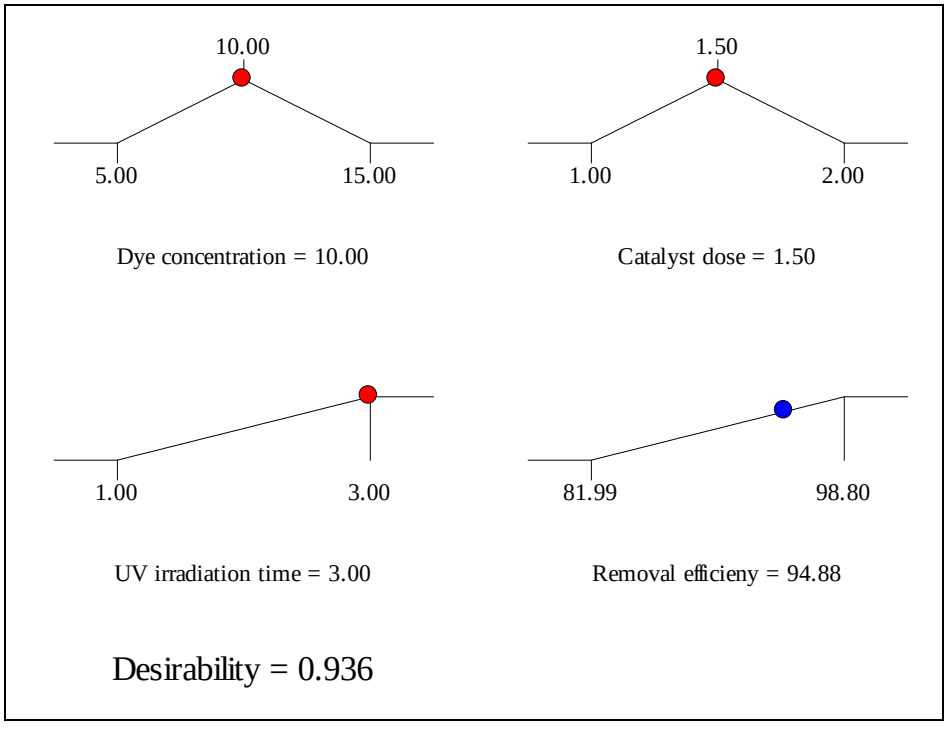

Figure 4.12: Optimization result for photocatalytic experiment

From the numerical optimization result in Figure 4.12, dye concentration 10mg/L, catalyst dose, 1.5g/L and UV irradation time 3h were selected with 0.936 desirability to pridict the maximum dye removal efficiency of 94.88%.

To validate the optimum conditions predicted by the model using desirability ramp, triplicate experiments were conducted using the optimized dye removal efficiency process conditions and mean percentage conversion value of 94.88% (94.5%, 95.01%, and 94.89) was obtained and results are closely related with the data obtained from optimization analysis using desirability functions.

4.4. Effect of process variables on photocatalytic performance

a) Effect of MO concentration

As shown in Fig. 4.13 an increase in methyl orange concentration (adsorbate) concentration results in adsorption capacity. However, an increase of methyl orange concentration reduces available adsorption sites, since more pollutants introduced to the system.

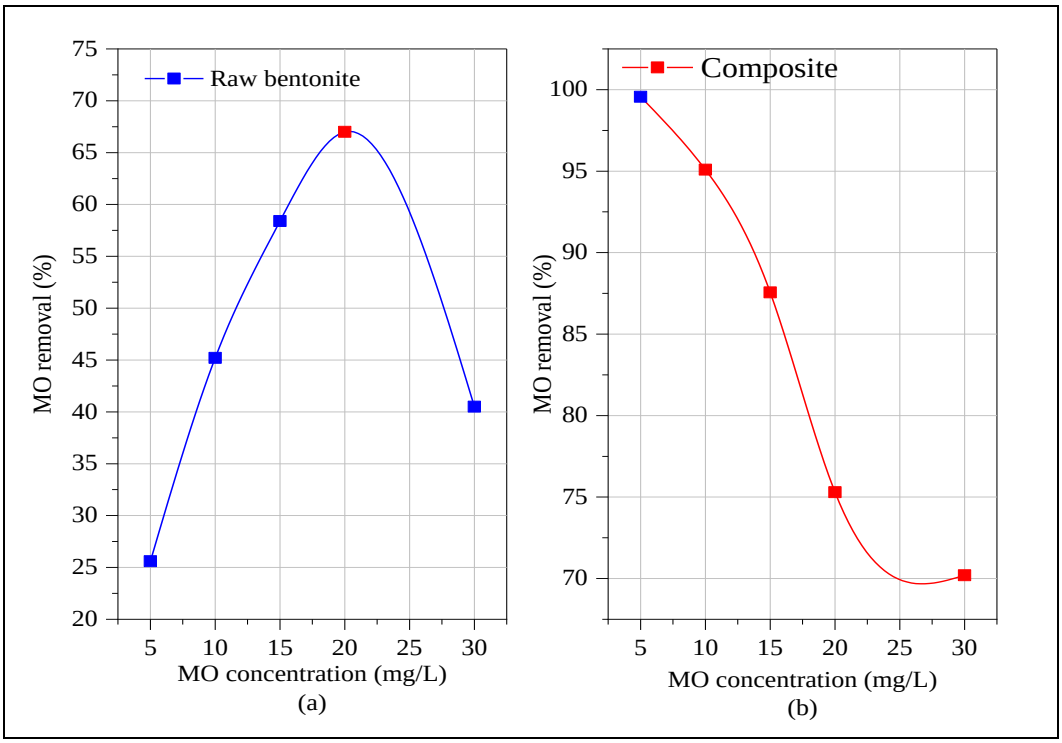

Figure 4.13 Effect of MO concentration on removal efficiency

From Fig. 4.13 (b), the composite titanium dioxide supported with bentonite has better adsorption and removal efficiency compared with raw bentonite. Even if the methyl orange removal efficiency increases to 30 mg/L, the composite can remove more than 70% and at minimum MO concentration it can remove up to 99.57% as shown in Appendix E (Table E1).

Also, bentonite had a maximum removal efficiency of 67% as shown in figure 4.13 (a). This justified that, the composite has efficient dye removal performance due to its adsorption and catalytic activity.

b) Effect of catalyst dose (composite)

As shown in Figure 4.14, the methyl orange removal performance of both bentonite and composite catalyst increases as the dosage increased. This was due to a finite surfaces were provided for adsorption of the model pollutant. Whereas, at lower catalyst dosage, limited surfaces were available and due to this the removal efficiency was reduced. But if the adsorbent dosage increased beyond the optimum value, its removal efficiency was decreased due to light scattering particles hindered light penetration into the solution.

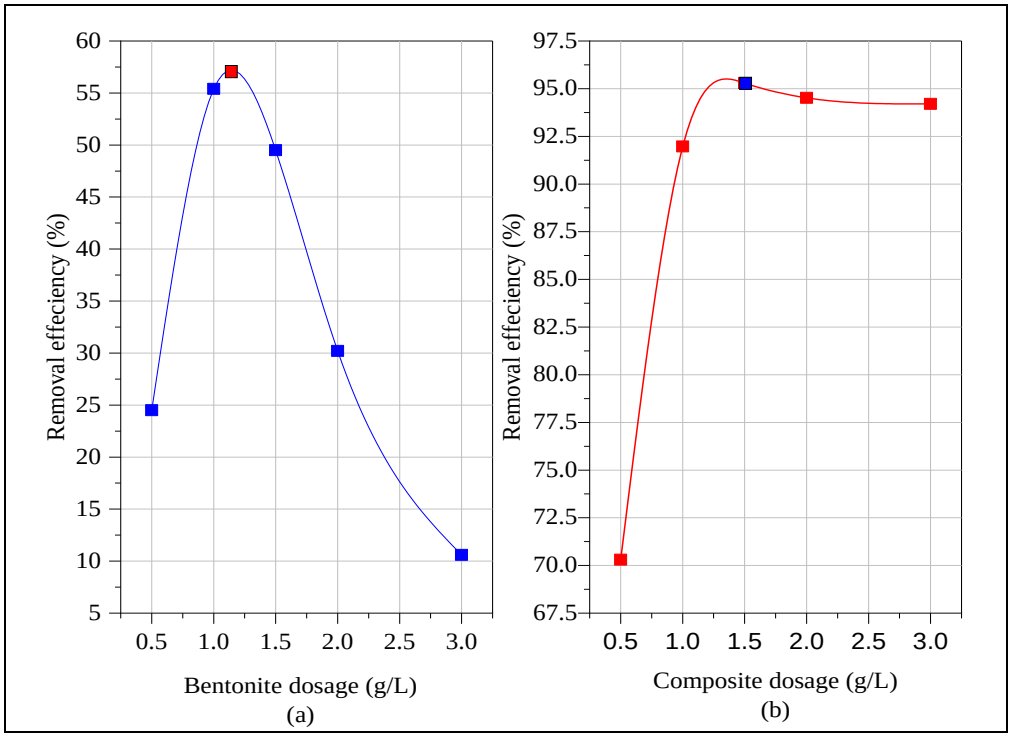

Figure 4.14: Effect of catalyst dose on dye removal efficiency

Based on H. Li, (2013) the optimum composite dosage for best removal efficieny should be maiantained below 2 g/L. As a result, the optimum composite dosage as shown in Fig. 4.14 (b) is 1.5 g/L with 95.29% removal efficiency. Also from Figure 4.14 (a), the optimum bentonite dosage was 1.14 g/L with removal efficiency of 55.4%.

c) Effect of UV irradiation time

As shown in the Figure below the percentage of dye removal increased for bentonite and composite with increase of contact time and UV irradiation time respectively. In the case of photocatalysis processes the photocatlytic efficiency was measured by the amount of hydroxyl radical generated via UV irradiation. As a result, when the exposure time is longer more hydroxyl radicals can be generated which was crucial for the degradation of organic pollutants in to carbon dioxide and water.

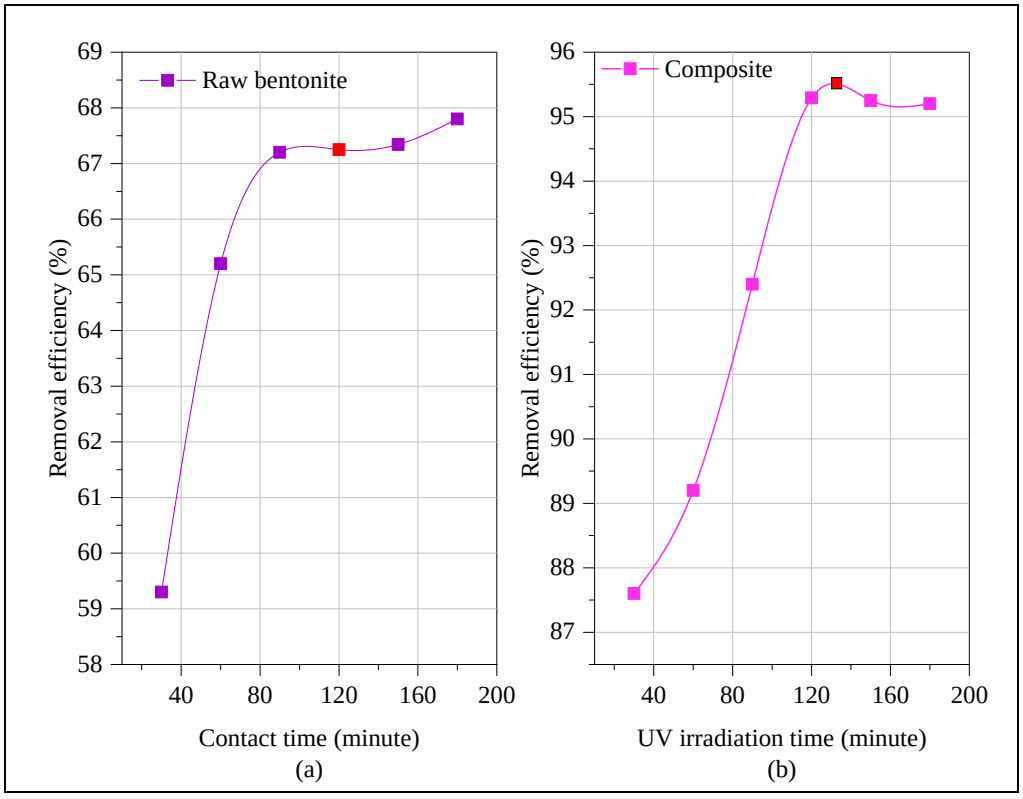

Figure 4.15: Effect of UV irradiation time on dye removal efficiency

As shown in Fig. 4.15(b) the composite catalyst had a removal efficiency of more than 95% at UV exposure time of 130 minutes whereas, raw bentonite was able to remove only 60% of

methyl orange at the same contact time. This result confirmed that, the presence of UV light during photocatalytic process of the composite plays a vital role for better removal efficiency.

4.5. Adsorption Isotherm

The experimental data obtained in Appendix Table D2 were plotted in a linearized fit of Langmuir and Freundlich adsorption isotherms in Fig. 4.16 (a) and (b) respectively.

The adsorption isotherm was selected based on the regression coefficient R^2 which was 0.9049 and 0.9549 for Langmuir and Freundlich isotherm respectively. As a result, the Freundlich isotherm model with constant terms n= 2.437 and K_F= 0.467 from slope and intercept respectively in Figure 4.16 (b). If 1/n value ranges from 0.1 to 1 justified that there was better adsorption process. Also the Langmuir constants based on Figure 4.13 were, q_m= 0.7698 and K_L= 1.603. The isotherm parameters calculated from the slope and intercept of linear isotherm model were summarized in Table 4.8.

Table 4.8: Constant parameters of Langmuir and Freundlich isotherm model

Isotherm model	Model equation	Parameters	
Langmuir Isotherm	Y = 1.299X + 0.810	R^2	0.9049
		q_m	0.7698
		K_L	1.603
Freundlich Isotherm	Y = 0.4103X – 0.3306	R^2	0.9549
		n	2.437
		KF	0.467

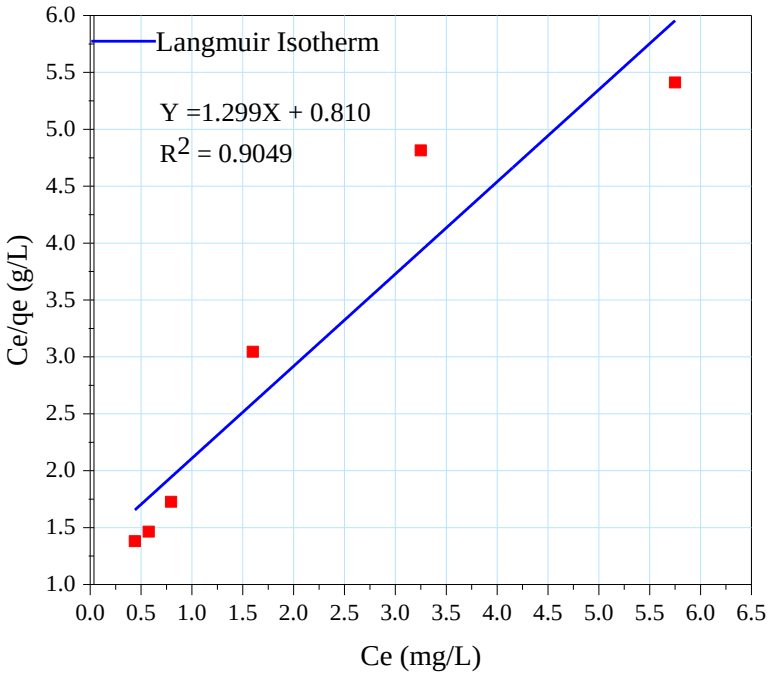

(a)

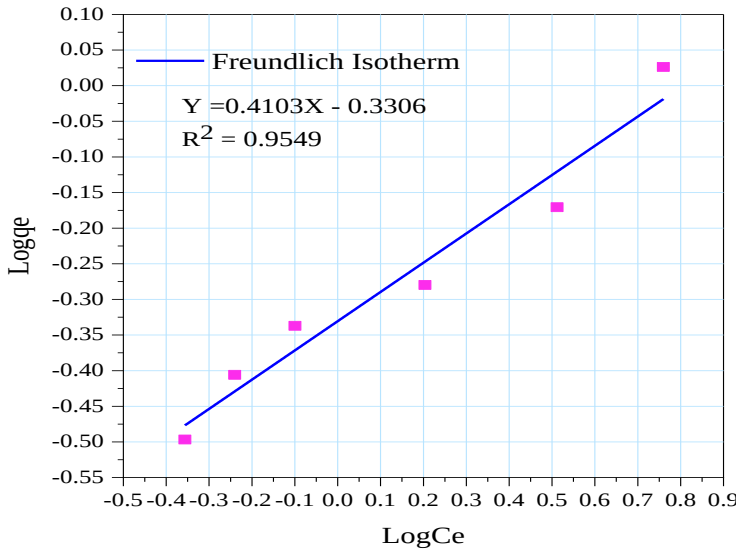

(b)

Figure 4.16: Langmuir and Freundlich Isotherm plot

Chapter 5

CONCLUSION AND RECOMMENDATION

5.1. Conclusion

In this study the impregnation synthesis parameters for the preparation of TiO_2 supported with clay bentonite composite catalyst were investigated and optimized using Box-Bhenkon response surface methodology. The study shown that, RSM optimize the process parameters with a limited number of trials and used as better tool to identify the interaction effect of the individual impregnation synthesis parameters and the photocatalytic process parameters. From the numerical optimization for catalyst synthesis calcination temperature, calcination time and TiO_2-bentonite ratio were used as constraint 96.54% MO removal efficiency was obtained. The photocatalytic optimization was done by taking MO concentration, catalyst dose and UV irradiation time as constraints 94.88% MO removal efficiency was obtained.

From crystal structure study in XRD result for bentonite supported TiO_2 composite the intensities of bentonite was decreased compared with raw bentonite which justified that, the bentonite was affected powder TiO_2 during impregnation process. From FTIR analysis the desired functional groups were determined for raw benitonite and composite which justified that, the impregnation of TiO_2 on to the bentonite surface.

In summary, the result of the study indicated that bentonite supported TiO_2 catalyst shows high photocatalytic and adsorption ability for the removal of dye effluents in wastewater. Therefore, it can be utilized as potential catalyst for real waste water treatment.

5.2. Recommendation

Porous material supported TiO_2 composite activated with visible light for water disinfection is an important research topic in practical application of photocatalysis. All experiments were performed under controlled parameters with artificially synthesized MO solution.

Considering the promising results obtained in this thesis with the above limitation the following recommendations are suggested for future work

- Further analysis on specific surface area and surface morphology should be required using BET (Brunauer-Emmett-Teller) and SEM (Scanning electron microscope) analysis respectively
- Proper photocatalytic reactor modified with UV lamp should be designed which may improve the photocatalytic performance.
- The performance of bentonite supported TiO_2 composite should be investigated in real waste water which has variety of minerals.
- The economic feasibility of this treatment methodology needs further investigation to confirm its advantage compared with the existing technologies.
- Regeneration studies have to be further studied at different process variables to confirm its reusability cycles.

REFERENCES

A. E. Segneanu, C. Orbeci, C. Lazau, P. Sfirloaga, P. Vlazan, C. Bandas, and I. G. (2013). *Waste water treatment methods. In: Water Treatment*. 53–80.

Abdullahi, S. L., & Audu, A. A. (2017). Comparative Analysis on Chemical Composition of Bentonite Clays Obtained from Ashaka and Tango Deposits in Gombe State , Nigeria. *ChemSearch Jorunal*, *8*(2), 35–40.

Abu-jdayil, B. (2011). International Journal of Mineral Processing Rheology of sodium and calcium bentonite – water dispersions : Effect of electrolytes and aging time. *International Journal of Mineral Processing*, *98*(3–4), 208–213.

Ademe, A. S., & Alemayehu, M. (2014). *Intellectual Properties Rights : Open Access Source and Determinants of Water Pollution in Ethiopia : Distributed Lag Modeling Approach*. *2*(2).

Al-qaradawi, S., & Salman, S. R. (2002). *Photocatalytic degradation of methyl orange as a model compound*. *148*(July 2001), 161–168.

Anandan, S., Ikuma, Y., & Niwa, K. (2010). *An Overview of Semi-Conductor Photocatalysis : Modification of TiO 2 Nanomaterials*. *162*, 239–260.

Anocomposites, C. L. A. Y. E. N., Praneeth, N. V. S., & Paria, S. (2017). *FOR P HOTOCATALYTIC A PPLICATIONS*.

Asamoah, R. B., Nyankson, E., Annan, E., & Efavi, J. K. (2018). *Industrial Applications of Clay Materials from Ghana (A Review)*.

Azami, M., Bahram, M., & Nouri, S. (2013). Central composite design for the optimization of removal of the azo dye, Methyl Red, from waste water using Fenton reaction. *Current Chemistry Letters*, *2*(2), 57–68.

Bagheri, S., Julkapli, N. M., Bee, S., & Hamid, A. (2014). *Titanium Dioxide as a Catalyst Support in Heterogeneous Catalysis*. *2014*.

Barka, N., & Assabbane, A. (2008). *Photocatalytic degradation of methyl orange with immobilized TiO2 nanoparticles : effect of pH and some inorganic anions*. (November 2014), 1–5.

Chaker, H., Chérif-aouali, L., Khaoulani, S., Bengueddach, A., & Fourmentin, S. (2016). Journal of Photochemistry and Photobiology A : Chemistry Photocatalytic degradation of methyl

orange and real wastewater by silver doped mesoporous TiO 2 catalysts. *"Journal of Photochemistry & Photobiology, A: Chemistry," 318*, 142–149.

Cheng, W., Huisheng, S. H. I., & Yan, L. I. (2012). *Preparation of Bentonite Supported Nano Titanium Dioxide Photocatalysts by Electrostatic Self-assembly Method*. (Iii), 603–607.

Cherrak, R., Hadjel, M., & Benderdouche, N. (2015). Heterogenous photocatalysis treatement of azo dye methyl orange by nano composite Tio2/diatomite. *Oriental Journal of Chemistry*, *31*(3), 1611–1620.

Dhahir, S. A. (2013). *Adsorption Study of Rhodamin B Dye on Iraqi Bentonite and Modified Bentonite by Nanocompounds TIO 2 , ZNO , AL 2 O 3 and Sodium Dodecyl Sulfate*. *9*(3), 269–279.

Divya, N., Bansal, A., & Jana, A. K. (2009). *Surface Modification , Characterization and Photocatlytic Performance of Nano-Sized Titania modified with Silver and Bentonite clay*. *4*(2), 43–53.

Environment, M. (n.d.). *Global good practices in industrial wastewater treatment and disposal / reuse , with special reference to common effluent treatment plants Central Pollution Control Board*.

Fischer, K., Gawel, A., Rosen, D., Krause, M., Abdul Latif, A., Griebel, J., … Schulze, A. (2017). Low-Temperature Synthesis of Anatase/Rutile/Brookite TiO2 Nanoparticles on a Polymer Membrane for Photocatalysis. *Catalysts*, *7*(7), 209.

Ghosh, S., & Das, A. P. (2015). Modified titanium oxide (TiO<inf>2</inf>) nanocomposites and its array of applications: a review. *Toxicological and Environmental Chemistry*, *97*(5), 491–514.

Hadjltaief, H. B., Omri, A., Zina, M. Ben, Costa, P. Da, & Galvez, M. E. (2015). *Titanium Dioxide Supported on Different Porous Materials as Photocatalyst for the Degradation of Methyl Green in Wastewaters*. *2015*.

Hassaan, M. A., & Nemr, A. El. (2017). *Health and Environmental Impacts of Dyes : Mini Review*. *1*(3), 64–67.

Hassena, H. (2016). *Modern Chemistry & Applications Photocatalytic Degradation of Methylene Blue by Using Al 2 O 3 / Fe 2 O 3 Nano Composite under Visible Light*. *4*(1), 3–7.

Hendrix, Y., Lazaro, A., Yu, Q., & Brouwers, J. (2015). *Titania-Silica Composites : A Review on the Photocatalytic Activity and Synthesis Methods*. (December), 161–177.

Karimi, L., & Salem, A. (2011). The role of bentonite particle size distribution on kinetic of cation exchange capacity. *Journal of Industrial and Engineering Chemistry*, *17*(1), 90–95.

Kebede Kassahun, S., Kiflie, Z., Shin, D. W., & Park, S. S. (2017). Photocatalytic Decolorization of Methylene Blue by N-doped TiO 2 Nanoparticles Prepared Under Different Synthesis Parameters. *Nanotechnol. J. Water Environ. Nanotechnol. J. Water Environ. Nanotechnol*, *2*(23), 136–144.

Khataee, A., & Mansoori, G. A. (2011). *Nanostructured Titanium Dioxide Materials*.

Kibanova, D., Cervini-Silva, J., & Destaillats, H. (2009). Efficiency of clay - TiO2 nanocomposites on the photocatalytic elimination of a model hydrophobic air pollutant. *Environmental Science and Technology*, *43*(5), 1500–1506.

Kočí, K., Matějka, V., Kovář, P., Lacný, Z., & Obalová, L. (2011). Comparison of the pure TiO2 and kaolinite/TiO2 composite as catalyst for CO2 photocatalytic reduction. *Catalysis Today*, *161*(1), 105–109.

Konsowa, A. E. H., El-taweel, Y. A. E., & Abogaliel, S. I. (2018). *The Effect of Graphene / TIO 2 Nanomaterials on Photocatalytic Performance for Industrial Wastewater Treatment*. *6*(5), 107–120.

Konstantinou, I. K., & Albanis, T. A. (2004). *TiO 2 -assisted photocatalytic degradation of azo dyes in aqueous solution : kinetic and mechanistic investigations A review*. *49*, 1–14.

Krasner, S. W. (2009). The formation and control of emerging disinfection by-products of health concern. *Philosophical Transactions of the Royal Society A: Mathematical, Physical and Engineering Sciences*, *367*(1904), 4077–4095.

Laysandra, L., Sari, M. W. M. K., Soetaredjo, F. E., Foe, K., Putro, J. N., Kurniawan, A., … Ismadji, S. (2017). Adsorption and photocatalytic performance of bentonite-titanium dioxide composites for methylene blue and rhodamine B decoloration. *Heliyon*, *3*(12), e00488.

Laysandra, L., Winda, M., Kartika, M., & Edi, F. (2017). Adsorption and photocatalytic performance of bentonite-titanium dioxide composites for methylene blue and rhodamine B decoloration. *Heliyon*, (July), e00488.

Lemeyonouin, P., & Guillaume, A. (2018). *“ Titanium Oxide-Clay ” as Adsorbent and Photocatalysts for Wastewater Treatment*. (January), 0–11.

Lemeyonouin, P., Guillaume, A., Chelaru, A., Visa, M., & Lassiné, O. (2018). *“ Titanium*

Oxide-Clay " as Adsorbent and Photocatalysts for Wastewater Treatment. *8*(1), 1–11.

Letters, M. S. (2011). *syntheses and its applications*. *46*(11), 3669–3686.

Leu, C. C. Æ. W. L. Æ. H. (2006). *Sustainable Water Quality Management Framework and a Strategy Planning System for a River Basin*. 952–973.

Li, F., Sun, S., Jiang, Y., & Xia, M. (2008). *Photodegradation of an azo dye using immobilized nanoparticles of TiO 2 supported by natural porous mineral*. *152*, 1037–1044.

Li, H. (2013). *Synthesis of Titanium Dioxide Photocatalyst with Tunable Nanoporosity Using Supercritical Fluids*. (January), 168–172. Retrieved from

Lin, M., Song, M., & Shen, X. (2012). *Photocatalyst Tio 2 Supported on Bentonite for Water Organic Pollutants Purification : A Literature Review*. *464*, 967–974.

Mittal, A., Malviya, A., Kaur, D., Mittal, J., & Kurup, L. (2007). *Studies on the adsorption kinetics and isotherms for the removal and recovery of Methyl Orange from wastewaters using waste materials*. *148*, 229–240.

Moradi, S. E., & Nasrollahpour, A. (2017). Competitive adsorption and photodegradation of Methyl orange and Rhodamine B by TiO 2 modified mesoporous carbon photo-catalyst on UV irradiation. *Materials Technology*, *7857*(June), 0.

Padhi, B. S. (2012). *Pollution due to synthetic dyes toxicity & carcinogenicity studies and remediation*. *3*(3), 940–955.

Paz, Y. (2010). *Composite Titanium Dioxide Photocatalysts and the " Adsorb & Shuttle " Approach : A Review*. *162*, 135–162.

Pirilä, M. (2015). *Adsorption and photocatalysis in water treatment : active, abundant and inexpensive materials and methods*.

Reddy, K. V., Reddy, D. N., & Reddy, K. H. (2011). Journal of Chemical and Pharmaceutical Research. *Journal of Chemical and Pharmaceutical Research*, *3*(2), 234–244.

Reza, K. M., Kurny, A., & Gulshan, F. (2015). Parameters affecting the photocatalytic degradation of dyes using TiO2: a review. *Applied Water Science*, *7*(4), 1569–1578.

Reza, K. M., Kurny, A., & Gulshan, F. (2017). Parameters affecting the photocatalytic degradation of dyes using TiO2: a review. *Applied Water Science*, *7*(4), 1569–1578.

Rossetto, E., Petkowicz, D. I., João, H. Z., Pergher, S. B. C., & Penha, F. G. (2010). Applied Clay Science Bentonites impregnated with TiO 2 for photodegradation of methylene blue. *Applied Clay Science*, *48*(4), 602–606.

Salem, A., & Saghapour, M. (2016). *Relationship between acidification factors and methylene blue uptake by Ca-bentonite : optimisation and kinetic study*. *70*(2), 2015–2016.

Santiago, F., Mucientes, A. E., Osorio, M., & Rivera, C. (2007). Preparation of composites and nanocomposites based on bentonite and poly(sodium acrylate). Effect of amount of bentonite on the swelling behaviour. *European Polymer Journal*, *43*(1), 1–9.

Segneanu, A. E., Orbeci, C., Lazau, C., Sfirloaga, P., Vlazan, P., Bandas, C., & Grozescu, I. (2013). *Waste Water Treatment Methods*.

Shan, A. Y., Ghazi, T. I. M., & Rashid, S. A. (2010). Immobilisation of titanium dioxide onto supporting materials in heterogeneous photocatalysis: A review. *Applied Catalysis A: General*, *389*(1–2), 1–8.

Silverstein, R.M.; Bassler, G.C.; and Morrill, T. C. 1981. (n.d.). *IR-frequencies*.

Sobota, I. (2016). *Bentonite processing BENTONITE PROCESSING*. (November).

Stojiljkovic, S., Miljkovic, V., Nikolic, G., Kostic, D., Arsic, B., Barber, J., … Savic, I. (2014). *The Influence of the Addition of Polymers on the Physico- Chemical Properties of Bentonite Suspensions*. *46*, 65–73.

Subramani, A. K., Byrappa, K., Ananda, S., Rai, K. M. L., Ranganathaiah, C., & Yoshimura, M. (2007). *Photocatalytic degradation of indigo carmine dye using TiO_2 impregnated activated carbon*. *30*(1), 37–41.

Sun, Z., Chen, Y., Ke, Q., Yang, Y., & Yuan, J. (2002). *Photocatalytic degradation of cationic azo dye by TiO 2 / bentonite nanocomposite*. *149*, 169–174.

Tulip, D. R. E. (2017). *STUDY ON VARIOUS TECHNOLOGIES IN WASTEWATER TREATMENT*. *8*(8), 1576–1580.

Turkar, S. S., Bharti, D. B., & Gaikwad, G. S. (2011). Various methods involved in waste water treatment to control water pollution. *Journal of Chemical and Pharmaceutical Research*, *3*(2), 58–65.

Ullah, I., Ali, S., Hanif, M. A., & Shahid, S. A. (2012). *Nanoscience for environmental remediation : A Review*. *2*, 60–77.

Verne, L. (2009). *The formation and control of emerging disinfection by-products of health concern*. 4077–4095.

Wang, X., Liu, Y., Hu, Z., Chen, Y., Liu, W., & Zhao, G. (2009). *Degradation of methyl orange by composite photocatalysts nano-TiO 2 immobilized on activated carbons of different*

porosities. *169*, 1061–1067.

Wu, E. M., & Kuo, S. (2015). *Decolourization of Methylene Blue in Water Using Bentonite Impregnated with Ti and Ag as Photocatalyst*. (August), 727–734.

Wu, H., Ma, J., Zhang, C., & He, H. (2014). Effect of TiO 2 calcination temperature on the photocatalytic oxidation of gaseous NH 3. *Journal of Environmental Sciences (China)*, *26*(3), 673–682.

Wu, X. P. (2017). A Review - The Properties and Applications of Nano-Structured Titanium Oxide Materials. *Key Engineering Materials*, *727*, 314–321.

Xing, B., Shi, C., Zhang, C., Yi, G., Chen, L., Guo, H., … Cao, J. (2016). *Preparation of TiO 2 / Activated Carbon Composites for Photocatalytic Degradation of RhB under UV Light Irradiation*. *2016*.

Yahya, N., Aziz, F., Jamaludin, N. A., Mutalib, M. A., Ismail, A. F., Salleh, W. N. W., … Ludin, N. A. (2018a). A review of Integrated Photocatalyst Adsorbents for Wastewater Treatment. *Biochemical Pharmacology*, (November).

Yahya, N., Aziz, F., Jamaludin, N. A., Mutalib, M. A., Ismail, A. F., Salleh, W. N. W., … Ludin, N. A. (2018b). PT SC. *Biochemical Pharmacology*.

Yang, C., Zhu, Y., Wang, J., Li, Z., Su, X., & Niu, C. (2015). Hydrothermal synthesis of TiO 2 - WO 3 -bentonite composites: Conventional versus ultrasonic pretreatments and their adsorption of methylene blue. *Applied Clay Science*, *105–106*, 243–251.

You, X., Chen, F., & Zhang, J. (2005). Effects of calcination on the physical and photocatalytic properties of TiO2 powders prepared by sol-gel template method. *Journal of Sol-Gel Science and Technology*, *34*(2), 181–187.

APPENDIX

Appendix A: Specific surface area calculation

The specific surface area of raw bentonite and composite catalyst was determined based on Blain's air permeability method using equation (3.1)

a) Surface area of the raw bentonite ($S_{Bentonite}$)

S_S= 377.4m^2/kg, (cement)

t_s= 37.8sec, (cement)

$t_{Bentonite}$= 5.84s

Then, $S_{Bentonite} = S_s \frac{\sqrt{t_{Bentonite}}}{\sqrt{t_s}} = 377.4 \frac{\sqrt{5.84}}{\sqrt{37.8}} cm^2 = 148.3 m^2/kg$

b) Surface area of the composite catalyst ($S_{composite}$)

S_S= 377.4m^2/kg, (cement)

t_s= 37.8sec, (cement)

$t_{composite}$= 1.41sec

Then, $S_{composite} = S_s \frac{\sqrt{t_{composite}}}{\sqrt{t_s}} = 377.4 \frac{\sqrt{1.41}}{\sqrt{37.8}} m^2/kg = 72.9 m^2/kg$

Appendix B: Crystal size of bentonite and composite catalyst

Crystal size of bentonite and composite catalyst was determined from equation (3.2) based on Scherer's method as follows from XRD plot .

Table B1: Average crystal size calculation for bentonite based on Scherer equation

2theta	Peak height	FWHM	Crystal size (nm) ($D= k\lambda/\beta\cos\theta$)
17.98	625.2	0.24	33.14052356
19.91	1000	0.44	18.12751992
20.56	402.1	1.92	4.158430285
21.1	309.8	2.48	3.222219655
21.63	352	0.88	9.088726979
22.22	797.3	0.2	40.03030165
26.74	558.9	0.08	100.9358959
28.64	209.4	0.2	40.53968587
28.82	239	0.56	14.48428494
28.96	268.4	0.64	12.67773851
34.74	618.6	0.2	41.15698701
35.26	248.3	1.16	7.106192393
35.85	249.5	1.12	7.372145227
36.06	221.4	0.88	9.388311398
36.23	201.1	0.4	20.66428633
36.43	131.9	1	8.270449282
36.62	594	0.36	22.98604356
36.88	126.4	0.16	51.75759161
Average crystal size (nm)			24.73

Table B2: Average crystal size calculation for composite based on Scherer equation

2theta	Peak height	FWHM	Crystal size ($D= k\lambda/\beta\cos\theta$)
19.94	304.4	0.16	49.85297226
20.14	186.2	0.4	19.94733925
22.06	51.4	0.32	25.01210487
23.18	224.2	0.2	40.09767404

25.67	1000	0.24	33.57225493
27.96	226.2	0.12	67.46513576
34.41	62.8	0.12	68.53352646
35.44	57.4	0.08	103.0913792
37.34	66.3	0.12	69.10317182
38.2	215	0.2	41.56848605
38.95	68.3	0.12	69.43967461
43.51	102.9	0.2	42.29226898
Average crystal size (nm)			53.42579266

Appendix C: Final dye concentration and respective removal efficiency after treatment

Sample	Final dye concentration(mg/L) $C = \frac{A + 0.0053}{0.048}$	$Removal\ efficiency\ (\%) = \left(\frac{C_o - C_t}{C_o}\right) * 100\%$
1	0.216	95.70
2	0.201	96.00
3	0.271	94.60
4	1.191	76.20
5	0.501	90.00
6	0.936	81.30
7	0.386	92.30
8	0.751	85.00
9	0.584	88.34
10	1.096	78.10
11	0.426	91.50
12	0.917	81.68
13	0.397	92.09
14	0.417	91.68
15	0.438	91.26

Appendix D: Standard methyl orange solution preparation

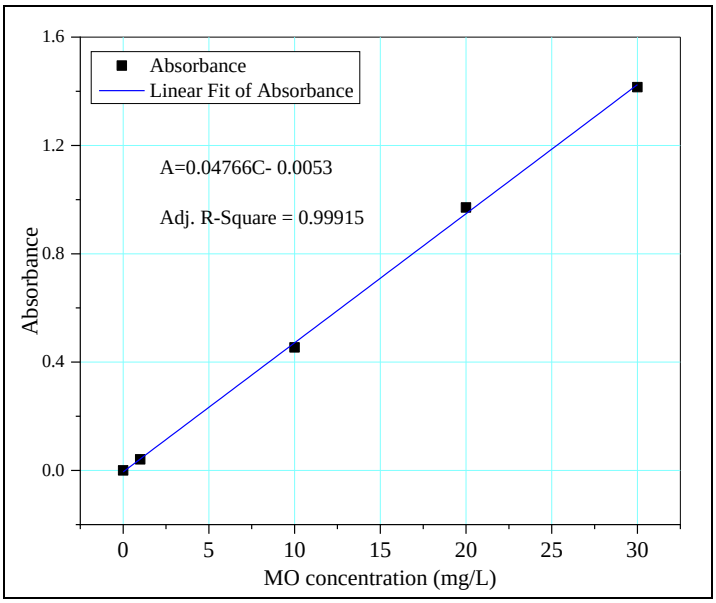

Figure D1: Standard curve of MO

Appendix E: Effect of process variables on MO removal efficiency

Table E1: Effect of MO concentration on bentonite and composite performance

MO concentration (mg/L)	Dye removal effeciency (%)	
	Bentonite	Composite
5	25.6	99.56
10	45.2	95.09
15	58.4	87.56
20	67	75.3
30	40.5	70.2

Table E2: Effect of bentonite and composite dose on dye remofal efficiency

Adsorbent Dosage (g/L)	Dye removal effeciency (%)	
	Bentonite	Composite
0.5	24.5	70.3
1	55.4	91.97
1.5	49.5	95.29
2	30.2	94.52

3	10.6	94.2

Table E3: Effect of UV irradiation time on MO removal efficiency

UV irradation time	MO removal efficiency (%)	
	Raw bentonite	Composite (TiO_2/bentonite)
30	59.3	87.6
60	65.2	89.2
90	67.2	92.4
120	67.15	95.29
150	67.34	95.25
180	67.5	95.2

Table F: Adsorption isotherm data

Catalyst dose (g/L)	Contact time (minute)	Dye concentration (mg/L)	Ce (mg/L)	qe (mg/g)	Ce/qe (g/L)	LogCe	Logqe
0.2	120	10	5.75	1.0625	5.4118	0.7597	0.026329
0.5	120	10	3.25	0.675	4.8148	0.5119	-0.1707
0.8	120	10	1.599	0.52506	3.0454	0.2038	-0.27979
1	120	10	0.795	0.46025	1.7273	-0.0996	-0.33701
1.2	120	10	0.575	0.39271	1.4642	-0.2403	-0.40593
1.5	120	10	0.44	0.31867	1.3808	-0.3565	-0.49666

Appendix G: Pictures of samples and some laboratory Equipment


Raw bentonite


Size reduction


Hammer mill


Bentonite powder

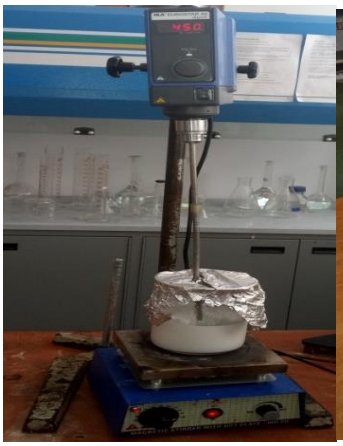
Mixing solution


Vacuum filter


Oven drier


Dried sample


Pestle & mortar


Muffle furnace


Desiccator

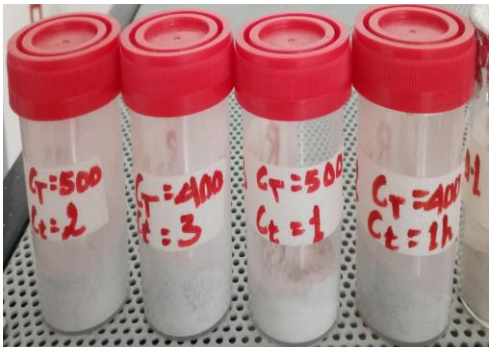

TiO_2/bentonite composite

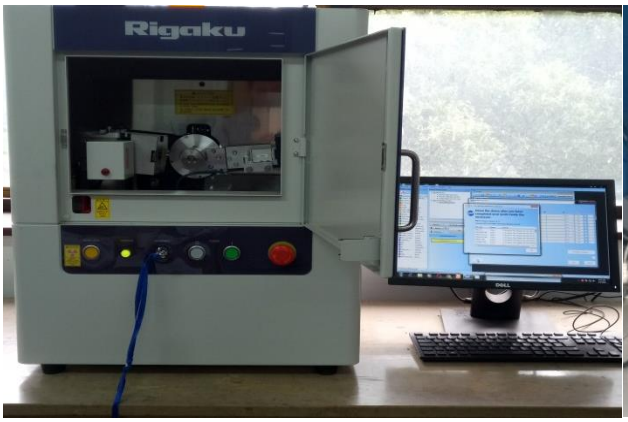

XRD apparatus

FTIR apparatus

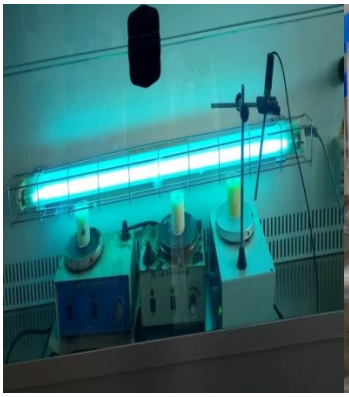

Microbial hood

Test tube

Centrifuge

UV-Vis spectrophotometer